STRESS SINGULAR ELEMENT APPLICATION TO FRACTURE PROBLEMS

STRESS SINGULAR ISOPARAMETRIC FINITE ELEMENT APPLICATION TO FRACTURE PROBLEMS

By

JAMES W. HOTCHKIES, P. ENG.

A Project

Submitted to the School of Graduate Studies

in Partial Fulfilment of the Requirements

for the degree

Master of Engineering

McMaster University

September 1984.

MASTER OF ENGINEERING (1984) MCMASTER UNIVERSITY
(Civil Engineering) HAMILTON, ONTARIO

TITLE: Application of a Stress Singular Isoparametric Finite Element to Fracture Problems

AUTHOR: James W. Hotchkies, B. Eng. (McMaster University)
P. Eng.

SUPERVISOR: Dr. Farooque A. Mirza

NUMBER OF PAGES: ix, 95

ABSTRACT

Stress singularity is developed in standard eight-node isoparametric finite elements, by shifting the mid-side nodes on the edges radiating from the corner node of interest to the quarter-points nearest that node. This feature is invaluable for use in the analysis of structural bodies with crack-like discontinuities; this analysis being particularly important for engineering development in Canada's northern and offshore regions. In these regions, extremely cold temperatures can lead to premature and sudden failure in structures that contain internal cracks, such as those imposed by welding. Consequently, a rational, cost-effective technique is required for the analysis of this type of problem.

The modified elements are used to investigate the fracture behaviour of three classical cracked body problems for which a number of results are available: the isotropic rectangular plates with a central crack or with symmetric edge cracks, and the orthotropic square plate with a central crack. The strain energy release-rate approach is used to determine the Mode I stress intensity factor for each specimen, and these are compared to data available in the literature. Good agreement is obtained between the results

of this analysis and those of other authors, even with the use of a very coarse finite element mesh.

The approach is then applied to the analysis of a standard ASTM E-399 bend bar specimen, and the results compared to values obtained from actual experiments on similar specimens. The objective of this phase is to investigate the possible practical application of the method to actual crack problems. When compared to the results obtained from an E-399 analysis of a high strength steel alloy, the finite element approach again yields good agreement.

The proposed approach is therefore regarded as an appropriate analytical tool for use in the study of cracked body problems, in materials that exhibit plane-strain behaviour.

ACKNOWLEDGEMENT

In presenting this project report, the author wishes to express his appreciation to his supervisor, Dr. F. A. Mirza, for the advice and guidance received during the research and preparation of this report.

The support and interest of Dr. D. W. Hoeppner, of the University of Toronto is also gratefully acknowledged, particularly for stimulating the initial interest in the subject of fracture mechanics and for supplying the experimental data used in the analysis.

Finally, and most importantly, my extreme appreciation to my wife, Lorraine, for her unfailing support during the many hours spent on this report and the related programme work.

TABLE OF CONTENTS

LIST OF FIGURES

LIST OF TABLES

CHAPTER 1

INTRODUCTION

An assessment of the fracture characteristics of materials has been an important factor in the design of bridges, ships, Arctic and offshore structures, mechanical equipment, etc. Nowhere is this more apparent than in Canada, where the development of resources in frontier regions is placing new and very severe demands on materials and fabricated components. With the trend toward larger, more highly stressed equipment and the introduction of analytical techniques that enhance design optimization, the potential for sudden, catastrophic brittle fractures in these hostile environments is significant. Consequently, it has become essential, for such applications, to incorporate fracture control into the design process and attempt to ensure material integrity under all expected environmental conditions.

Over the last decade, considerable attention has been focused on the use of fracture mechanics as an approach to the material integrity problem. Realizing that all structures and components have inherent discontinuities, such as inclusions, surface cracks, weld defects and other

similar internal or external defects, an understanding of their effects on overall structural performance is essential to predict strength and life. Such predictions are dependent, however, on the knowledge of the crack tip stress intensity factor as a function of applied stress and geometry of the structure, and on the experimental determination of the critical stress intensity factor and crack growth rates for the material under consideration.

Principles of fracture mechanics have already been adopted by many design engineers. A number of recent publications [1-5] discuss the concepts and application of the approach in detail, and therefore no attempt will be made to perform such a development. However, for the purposes of this study, Chapter 2 will review some of the fundamental concepts of linear elastic fracture mechanics and, specifically, the use of the finite element method in such problems. At this point, it is sufficient to note that the successful application of fracture mechanics to practical problems depends on the reasonably accurate determination of the stress intensity factor for the crack configuration and material properties under investigation.

The theoretical determination of a stress intensity factor requires the exact solution of the elasticity problem for the specific crack configuration, using very

sophisticated mathematical approaches. In most practical cases, however, an exact solution to such a complex, real problem may be extremely difficult, or impossible to obtain. As most real situations rarely conform to idealized models, for which exact solutions may exist, it becomes necessary to adopt an approximate approach that provides consistently accurate crack property predictions. The finite element method has been shown to be such an approach, and has received considerable attention [6-18].

The finite element method is now a well established numerical technique for determining stresses in structures. It has also become a very reliable numerical tool to use in the analysis of stress singular problems. However, as the method typically utilizes polynomial representations of displacements and/or stresses, it is very difficult to accurately model the crack behaviour in the neighbourhood of the stress singularity. Two distinct approaches were developed in response to this problem, though neither one was completely satisfactory. The simplest approach utilized an extremely refined mesh in the region of the crack tip [6,7]. This method, however, results in an expensive and demanding use of computer time and requires a very tedious effort of data preparation. The other basic approach to the problem involved the development of special crack tip elements [17,18], which include stress singularities. This

technique also has some detractions however, in that the special elements normally lack the constant strain and rigid body modes [12]. They also require the use of special, sophisticated programmes.

Recently, several authors [11,12,14] have proposed modifications to standard eight-node, isoparametric, displacement type elements. These allow the development of the necessary singularity in a very simple manner. This approach, discussed in Chapter 3, provides a simple method of modelling crack-tip behaviour, without the need for either extensive mesh refinement or special elements.

Special methods have also been proposed [26] to allow the degeneration of an eight-node, quadrilateral, isoparametric element to a six-node, triangular, isoparametric element. Such an approach greatly enhances mesh generation flexibility, and eases the transition to coarse mesh configurations for regions of regular stress distribution. This procedure is developed in Chapter 4.

In the investigation presented in this report, both of these features are incorporated into an existing finite element programme, that is based on standard eight-node, quadrilateral, isoparametric elements. This is then used to evaluate the fracture characteristics of several standard

crack models: the double-edge notched strip, the centre cracked strip and the orthotropic plate with a central crack. In Chapter 5, the results of these analyses are compared to those of other authors. The approach is then used to model specimens for which experimental data is available, in order to assess its potential for practical applications. The results are discussed in Chapter 6.

Finally, in Chapter 7, several conclusions are presented and discussed, specifically in relation to future research that should be undertaken.

CHAPTER 2

FRACTURE MECHANICS: THE BASIC THEORY AND THE USE OF FINITE ELEMENT METHODS

Fracture mechanics is now well established as a design tool for many applications: aerospace equipment, off-highway equipment, pressure vessels, offshore structures, bridges, etc. In the future, due to trends in engineering design and in project requirements, even greater use will be made of this analytical procedure. Extensive literature is available on the subjects of fracture and fatigue, and no attempt will be made here to discuss them in detail. However, certain basic information, pertinent to the development of a finite element model for a cracked body, will be presented in this chapter. A review of the general concepts of fracture and fracture mechanics, and an outline of linear elastic fracture mechanics is presented. Finally, details of various finite element approaches to the problem of determining the stress intensity factors are discussed.

2.1 Fracture Mechanics Theory

The basic purpose of fracture mechanics is to

provide a correlation between experimental data and actual service conditions, by developing a quantitative relationship between applied stress, discontinuity size and material toughness. It attempts therefore, to provide a method by which the strength and life of a cracked structure can be predicted with reasonable accuracy.

One of the earliest approaches to the problem was developed by Griffith who, in 1920 [19], proposed an energy balance argument for coplanar growth of a sharp crack. This concept, which is valid for brittle materials, suggests that a crack will begin to propagate if the energy released during crack growth is equal to the energy required to form the new crack surface. For example, when a pre-existing discontinuity in a brittle material, subject to an applied tensile stress, grows by increasing its area by dA, a small amount of energy, dQ, is absorbed in the process and the stored strain energy of the specimen is decreased by dU. When the rate of energy absorption equals the rate of energy release, ie $-dU/dA = dQ/dA$, it is possible for the crack to grow without the need for additional work to be done by the applied stress. Griffith associated the energy absorbed with the surface energy of the growing crack surface. This gives the following relationships for infinitely long plates:

$$\sigma_c = (2\gamma E/\pi a)^{\frac{1}{2}} \qquad \text{(plane stress)} \qquad (2.1.1.a)$$

$$\sigma_c = (2\gamma E/(1-\nu^2)\pi a)^{\frac{1}{2}} \qquad \text{(plane strain)} \qquad (2.1.1.b)$$

where:

σ_c = fracture stress

γ = surface energy of the solid

E = modulus of elasticity

a = half of the crack length

ν = Poisson's ratio

Griffith's theory was essentially developed for glass, however, and was not particularly relevant for most metals. For such materials, it was postulated [20] that energy, far in excess of the surface energy, is absorbed through plastic deformation at, or near the crack tip. Modifications to Equations (2.1.1.a) and (2.1.1.b) were proposed to accomodate this plasticity effect:

$$\sigma_c = (E\,\gamma_p/\pi a)^{\frac{1}{2}} \qquad (2.1.2)$$

where γ_p = energy term to account for plastic deformation at crack tip.

Irwin [21] also developed similar relationships, based on the strain energy release rate, G, such that:

$$\sigma_c = (EG_c/\pi a)^{1/2} \qquad \text{(plane stress)} \qquad (2.1.3.a)$$

$$\sigma_c = (EG_c/(1-\nu^2)\pi a)^{1/2} \qquad \text{(plane strain)} \qquad (2.1.3.b)$$

where G_c = critical value of G

Regarding linear elastic fracture mechanics, the limiting solution for the elastic state of stress around a sharp crack is of the following form [6]:

$$\sigma = (K/r^{1/2})f(\theta) \qquad (2.1.4)$$

where: σ = one of the stress components

r, θ = polar coordinates (origin at the crack tip)

f = a trigonometric function of θ, which depends on the stress component considered and the symmetry of the problem.

K = constant

In the above equation the constant, K, is dependent on geometry, such as crack length, and the loading. Furthermore, since it represents the intensity of the stress field around the crack tip, K is also referred to as the stress intensity factor.

Irwin related this stress intensity factor to the

strain energy release rate in the following manner:

$$G = K^2/E \qquad \text{(plane stress)} \qquad (2.1.5.a)$$

$$G = K^2(1-\nu^2)/E \qquad \text{(plane strain)} \qquad (2.1.5.b)$$

In the case of the idealized, linear elastic theory, it is assumed that, for a given material the behaviour of the crack, whether it remains stable, grows without bound or grows at a definite rate, depends only on the magnitude of the stress intensity factor. It is therefore possible to characterize materials by determining the value of K, as a function of applied stress and crack length, at which unstable crack growth begins to occur. This limit is defined as the critical stress intensity factor, K_c. Then, for any other structural configuration of this material, in a similar environment, unstable crack growth will initiate whenever the crack length and stress conditions combine to produce a stress intensity factor equal to the value of K_c.

Combining Equations (2.1.3.a) with (2.1.5.a) and (2.1.3.b) with (2.1.5.b), it is shown that:

$$K_c = (EG_c)^{1/2} \qquad \text{(plane stress)} \qquad (2.1.6.a)$$

$$K_c = (EG_c/(1-\nu^2))^{1/2} \qquad \text{(plane strain)} \qquad (2.1.6.b)$$

In actual practice, materials that exhibit plane stress behaviour have significant zones of plastic deformation around the crack tip, and are not realistically represented by Equation (2.1.6.a). However, very high strength, very thick or brittle materials tend more toward the plane strain condition, and Equation (2.1.6.b) may be sufficiently accurate.

In his early papers, Irwin also concluded that fracture behaviour could be characterized by three basic modes of crack extension: Modes I, II and III. These three modes are illustrated in Figure 2.1.

Mode I is defined as the opening mode, with in-plane crack propagation. This is the most frequently analyzed crack mode for modelling purposes. Mode II is the sliding mode, characterized by a shear displacement perpendicular to the crack front. Mode III is the tearing mode, characterized by a shear displacement parallel to the crack front.

In the case of plane stress or plane strain, where the material contains a straight crack, subject to in-plane stresses, only Modes I and II are pertinent. For these cases, non-zero stress components are mathematically infinite at the crack tip, and the stress state in the neighbourhood of the crack can be expressed as:

$$\tau_{11} = (K_I / \sqrt{2r})\cos(\theta/2)(1-\sin(\theta/2)\sin(3\theta/2)) - (K_{II}/\sqrt{2r})\sin(\theta/2)(2+\cos(\theta/2)\cos(3\theta/2) + \ldots . \quad (2.1.7.a)$$

$$= (K_I / \sqrt{2r})\cos(\theta/2)(1+\sin(\theta/2)\sin(3\theta/2)) + (K_{II}/\sqrt{2r})\sin(\theta/2)\cos(\theta/2)\cos(3\theta/2)) + \ldots . \quad (2.1.7.b)$$

$$= (K_I / \sqrt{2r})\cos(\theta/2)\sin(\theta/2)\cos(3\theta/2) + (K_{II}/\sqrt{2r})\cos(\theta/2)(1-\sin(\theta/2)(3\theta/2)) + \ldots . \quad (2.1.7.c)$$

where the non-singular stress terms have been dropped, and r and θ are the polar coordinates.

The stress intensity factors K_I and K_{II} are the symmetric and skew-symmetric components, associated with the Mode I and Mode II conditions respectively. Similar to the previous discussion on the generalized stress intensity factor, critical values of K_I and K_{II} exist, for which there are associated crack instabilities. These are denoted as K_{Ic} and K_{IIc}. K_{Ic} is also frequently referred to as the fracture toughness of a given material, because the standard material evaluation test procedures are usually based on specimens that exhibit Mode I behaviour. For the purposes of this study only Mode I behaviour will be discussed. Therefore, only the first terms in Equations (2.1.7.a), (2.1.7.b) and (2.1.7.c) will be retained.

Finally, considering Equations (2.1.6.a) and (2.1.6.b), it is important to note that:

$$K_{Ic} = (EG_{Ic})^{1/2} \qquad \text{(plane stress)} \qquad (2.1.8.a)$$

$$K_{Ic} = (EG_{Ic}/(1-\nu^2))^{1/2} \qquad \text{(plane strain)} \qquad (2.1.8.b)$$

Once determined, K_{Ic} can then be used to predict the allowable defect size for a given applied stress, or conversely the allowable stress for the largest anticipated discontinuity.

2.2 The Application of the Finite Element Method to Linear Elastic Fracture Mechanics

The determination of the crack tip stress intensity factor is essential to the solution of any fracture problem. This requires the exact solution of the elasticity problem formulated for the cracked body however, and in most cases this is almost impossible to accomplish. For a number of basic crack profiles, very sophisticated mathematical solutions have been derived, and tables of stress intensity factors prepared [22]. In most practical cases however, such rigorous solutions are very difficult or impossible to achieve. Other approximate solution techniques must be adopted therefore: the alternating method, the

boundary-integral equation method, the line-spring model, the finite element method, etc. [23]. Of these, the finite element method has been particularly successful and has received considerable attention in recent years.

Two basic approaches predominate: the direct approach which uses special crack tip elements with an inherent singularity, and the indirect approach that uses standard polynomial functions for finite elements. The latter attempts to define crack tip behaviour in terms of the solution distant from the crack tip.

Using special elements, Tong and Atluri [17] achieved K_I results within 1 to 2 percent, while Mau and Yang [18] were able to reduce their error to below 1 percent. The use of such an approach however, can lead to extensive and sophisticated programming changes. Furthermore, their flexibility with respect to changing crack direction is not well understood.

With the indirect approach, the general tendency has been to develop extremely refined meshes around the crack tip. It is possible, therefore, to determine with some degree of accuracy the behaviour at some distance from the crack tip and use this to predict the approximate conditions at the tip. Two basic philosophies have evolved around this

subject. The first approach involves the extrapolation of a field parameter near the crack tip using calculated displacement or stress fields. The other technique considers the potential energy release rate due to crack extension, from which it is possible to determine the required fracture properties.

Chan, Tuba and Wilson [7] typify the extrapolation approach. They develop a graphical relationship between stress components and distances along a ray emanating from the crack tip, and then extrapolate back to the tip. Stress intensity factors can then be determined from the basic stress equations, (2.1.7.a) through (2.1.7.c). Similar techniques could also be applied to the relationship of displacement and distance from the crack tip. In their paper, these authors reported solutions within 5 percent of the accepted exact values for K_I. However, extremely refined mesh configurations were required. This implies very expensive solutions, both in terms of computer cost and data preparation.

A number of energy methods have been proposed, but the standard approach used by Mowbray [8] and the J-integral analogue proposed by Parks [10], appear to be the two most practical techniques. Mowbray analyzed the same basic specimen for various crack extensions, and then used the

strain energy release rate concept to predict K_I . By this approach, he was able to achieve an accuracy of five percent, with a significantly less refined mesh than that of Chan et al.

Parks' technique was essentially a finite element model of the J-integral approach of Rice [24], which considers the energy function along a path-independent integral surrounding the crack tip. By this approach, Parks was able to determine the potential energy release rate without the need for multiple analyses for various crack extensions, using the stiffness derivative technique.

In this study, the basic energy approach, similar to that of Mowbray, will be used for determination of crack tip properties. However, to eliminate the need for mesh refinement, element modifications are incorporated, as outlined in Chapter 3. By this method, it is possible to achieve significant improvements without expensive computational effort.

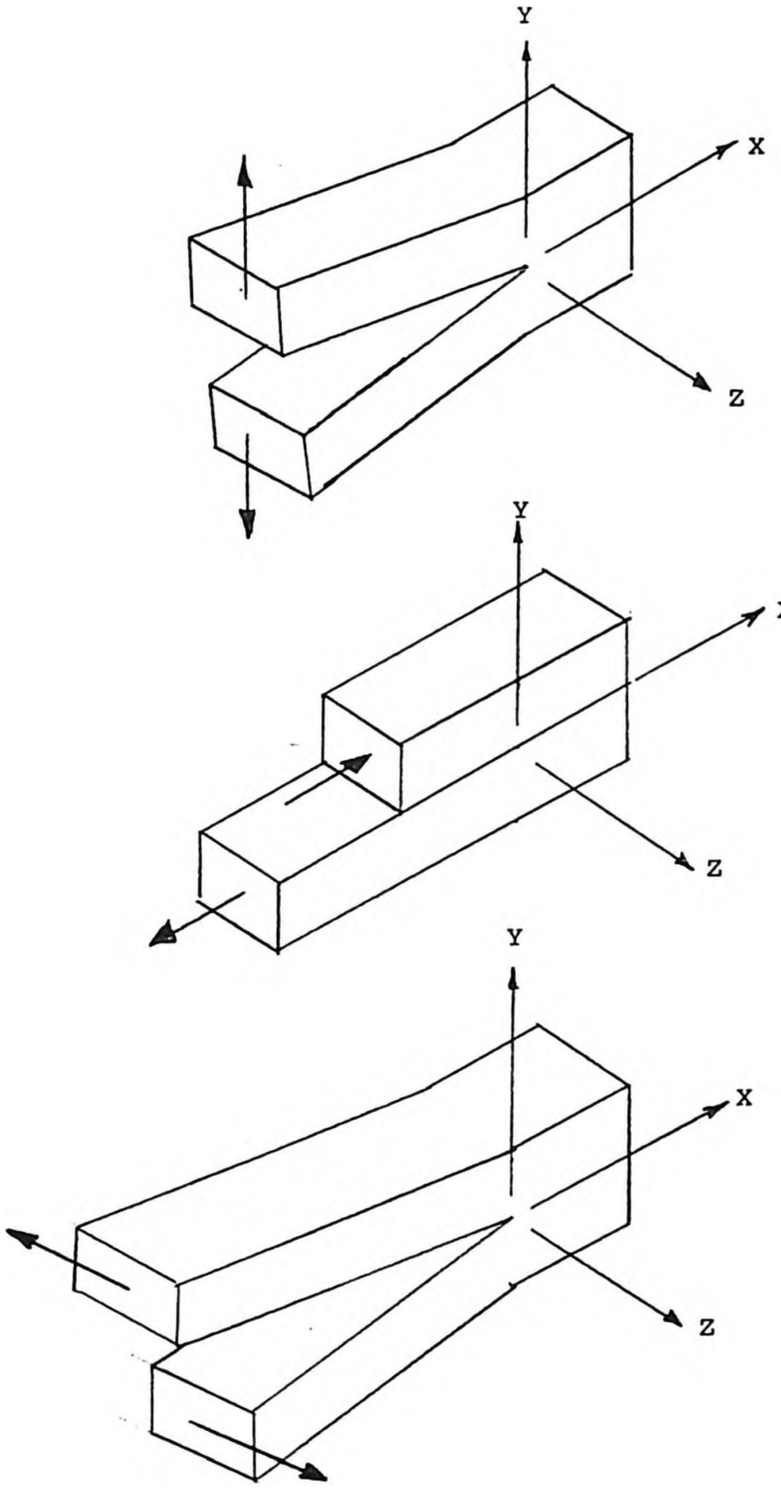

FIGURE 2.1: Three Primary Modes of Fracture

CHAPTER 3

DEVELOPMENT OF THE THEORY OF NODE SHIFTING

A significant problem with the use of the standard displacement finite element method in fracture analysis is the difficulty encountered in attempting to model the stress singularity at the crack tip. As previously stated, early techniques incorporated special crack tip elements or very refined mesh configurations, but both methods are less than satisfactory.

Recently however, several authors [11,12,14], have proposed a technique for use with eight-node, quadrilateral, isoparametric elements that eliminates the need for either special elements or meshes. As a result, the technique provides a cost-effective method of solving crack propagation problems using a standard, eight-node, isoparametric finite element programme. The technique involves the use of standard, eight-node, displacement-type, isoparametric elements where the mid-side nodes on the edges adjacent to the crack tip are displaced to the quarter point position nearer to the tip. This simple modification introduces the required singularity for modelling the crack tip behaviour.

3.1 Node-Shifting

For the eight-node, quadrilateral, isoparametric element, the shape functions have been formulated for the parent (square) element in the natural coordinate system (ξ, η) and subsequently mapped into a Cartesian coordinate system (x, y). Consider the eight-node element that is transformed from the $\xi\eta$ plane into the xy plane, in Figure 3.1. The transformation takes the form:

$$x = \sum_{i=1}^{8} N_i(\xi, \eta)\, x_i \qquad (3.1.1.a)$$

$$y = \sum_{i=1}^{8} N_i(\xi, \eta)\, y_i \qquad (3.1.1.b)$$

where the shape function corresponding to node i is:

$$\begin{aligned} N_i = {} & (1+\xi\xi_i)(1-\eta\eta_i) - (1-\xi^2)(1+\eta\eta_i) - (1-\eta^2)(1+\xi\xi_i)\xi_i^2\eta_i^2/4 \\ & + (1-\xi^2)(1+\eta\eta_i)(1-\xi_i^2)\eta_i^2/2 \\ & + (1-\eta^2)(1+\xi\xi_i)(1-\eta_i^2)\xi_i^2/2 \end{aligned} \qquad (3.1.2)$$

and (ξ_i, η_i) are the coordinates of node i in the transformed system.

The same shape functions are also used for displacements, such that:

$$u = \sum_{i=1}^{8} N_i(\xi,\eta)u_i \qquad (3.1.3.a)$$

$$v = \sum_{i=1}^{8} N_i(\xi,\eta)v_i \qquad (3.1.3.b)$$

The stiffness matrix of an element is then computed in the following manner:

$$[K] = \int_V [B]^T [D][B]dV \qquad (3.1.4)$$

where [B] and [D] are defined such that:

$$\{\varepsilon\} = [B]\{\delta\} \qquad (3.1.5)$$

$$\{\delta\}^T = \langle u_1\ v_1\ u_2\ v_2 \ldots\ldots\ldots u_8\ v_8 \rangle$$

$$\{\sigma\} = [D]\{\varepsilon\} \qquad (3.1.6)$$

$$[B] = \begin{bmatrix} \partial N_1/\partial x & 0 & \ldots\ldots & \partial N_8/\partial x & 0 \\ 0 & \partial N_1/\partial y & \ldots\ldots & 0 & \partial N_8/\partial y \\ \partial N_1/\partial y & \partial N_1/\partial x & \ldots\ldots & \partial N_8/\partial y & \partial N_8/\partial x \end{bmatrix} \qquad (3.1.7)$$

and [D] is the elasticity matrix (plane stress or plane strain).

However, as the shape functions are defined in the natural coordinate system, the terms in (3.1.7) can be written as:

$$\begin{bmatrix} \partial N_i/\partial x \\ \\ \partial N_i/\partial y \end{bmatrix} = [J]^{-1} \begin{bmatrix} \partial N_i/\partial \xi \\ \\ \partial N_i/\partial \eta \end{bmatrix} \qquad (3.1.8)$$

where:

$$[J] = \begin{bmatrix} \partial x/\partial \xi & \partial y/\partial \xi \\ \\ \partial x/\partial \eta & \partial y/\partial \eta \end{bmatrix} \qquad (3.1.9)$$

is the Jacobian matrix of transformation which can be evaluated and inverted at any point within the element domain.

The stiffness matrix of (3.1.4) can therefore be rewritten as [32]:

$$[K] = \int_{-1}^{1}\int_{-1}^{1} [B]^T [D][B] \det[J] d\xi\, d\eta \qquad (3.1.10)$$

For an investigation of crack tip behaviour, it is important to obtain a singularity at the crack tip. To accomplish this, consider Equation (3.1.9). From this expression, it can be observed that a singularity condition can be achieved by requiring the Jacobian [J] to become singular at the crack tip. This requires that the determinant of the Jacobian matrix, det[J], vanish at the

crack tip, where:

$$\det[J] = \partial(x,y)/\partial(\xi,\eta) \qquad (3.1.11)$$

Of course, this will lead to singular values for x and y, and hence, the strains and stresses will also become singular as required.

To investigate the singularity requirement, consider Figure 3.2. For the edge n =-1, the non-zero shape functions are:

$$N_1 = -\xi(1-\xi)/2 \qquad (3.1.12.a)$$

$$N_2 = \xi(1+\xi)/2 \qquad (3.1.12.b)$$

$$N_5 = (1-\xi^2) \qquad (3.1.12.c)$$

and therefore the transformation of Equation (3.1.3.a) takes the form:

$$x = \sum_{i=1}^{8} N_i x_i$$
$$= -0.5\xi(1-\xi)x_1 + 0.5\xi(1+\xi)x_2 + (1-\xi^2)x_5 \qquad (3.1.13)$$

For the edge under study, (x=0, x=1, x=s), Equation (3.1.13) becomes:

$$x = 0.5\xi(1+\xi) + s(1-\xi^2)$$

or rearranging:

$$(0.5-s)\xi^2 + 0.5\xi + (s-x) = 0 \qquad (3.1.14)$$

the roots of which are:

$$\xi = [-0.5 +/- 0.5\sqrt{1-8(1-2s)(s-x)}]/(1-2s) \qquad (3.1.15)$$

For only the positive root:

$$\partial\xi/\partial x = 2/[\sqrt{1-8(1-2s)(s-x)}] \qquad (3.1.16)$$

which is singular for:

$$1-8(1-2s)(s-x) = 0 \qquad (3.1.17)$$

Therefore, for $\partial\xi/\partial x$ to be singular at x = 0, s must equal one quarter (s=1/4). Substituting for s = 1/4 into (3.1.16) gives:

$$\partial\xi/\partial x = 2/[\sqrt{1-8(1-2s)(s-x)}] = 1/\sqrt{x} \qquad (3.1.18)$$

Considering only the u displacements along the edge $\eta = -1$:

$$u = -0.5\xi(1-\xi)u_1 + 0.5\xi(1+\xi)u_2 + (1-\xi^2)u_5 \qquad (3.1.19)$$

and, in general:

$$\varepsilon_{xx} = \partial u/\partial x = (\partial u/\partial \xi)(\partial \xi/\partial x)$$
$$= \sum (\partial N_i/\partial \xi)(u_i/\sqrt{x}) \qquad (3.1.20)$$

Similarly, ε_{xx} and γ_{xy} strains can also be shown to vary as $(1/\sqrt{x})$. The strain singularity along the line $\eta = -1$ is therefore of the form $(1/\sqrt{r})$, i.e. the singularity required for the elastic analysis of crack tip behaviour.

From this analysis, it is therefore evident that the distorted, eight-node, quadrilateral, isoparametric elements, with the mid-side nodes shifted to the quarter-points, introduce the necessary singularity into the solution technique. Further refinements are possible, [12], where triangular crack tip elements, degenerated from regular quadrilateral isoparametric elements, are developed. As shown by both Barsoum and Heymann, the triangular element should provide more accurate results than the rectangular element, owing to a superior bounding on total strain energy.

However, from present results, the prediction of K_I using a quadrilateral element, strain energy release-rate approach yields results with acceptable variation for most engineering applications. Further investigation of this approach would, nevertheless, be valuable in order to explore the full potential of this finite element approach to fracture mechanics problems.

In the present analysis, distorted elements are used wherever a node of that element coincides with the crack tip. Also, all edges parallel to rays emanating from the crack tip are also subjected to the node-shifting operation. All other elements and edges are unchanged. It is obvious therefore, that only minimal effort is required to accomodate the presence of cracks for a linear elastic fracture analysis.

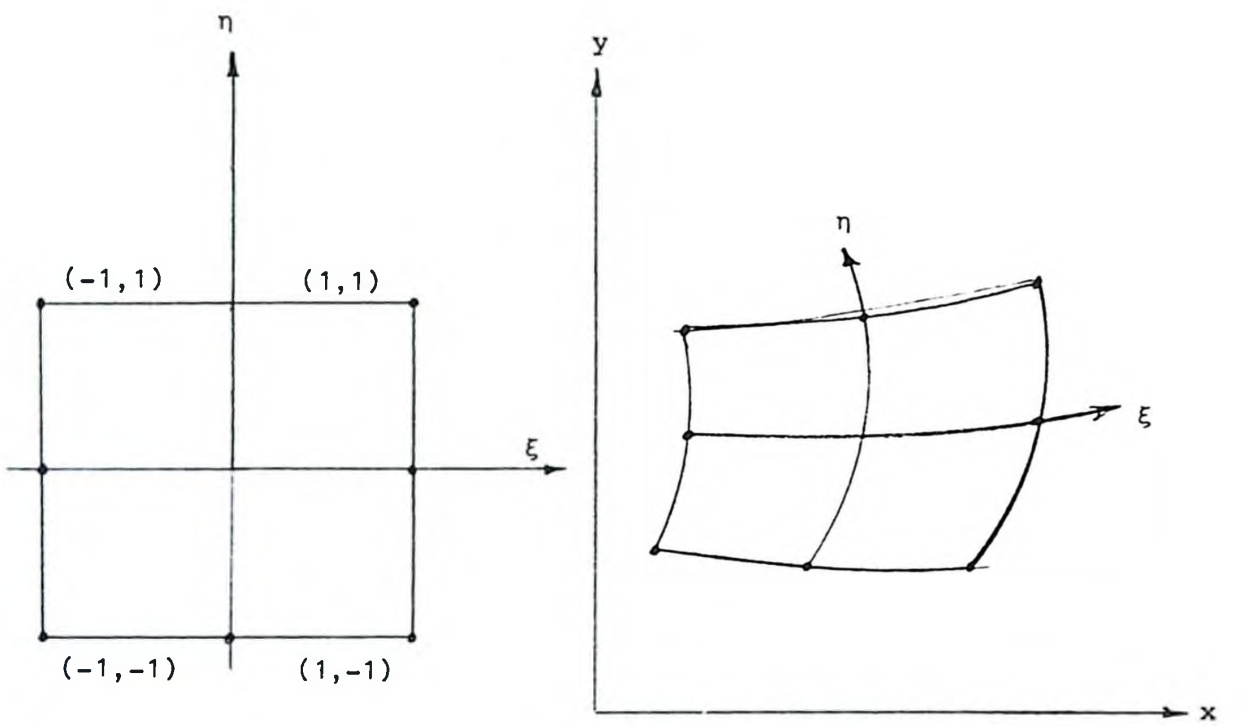

FIGURE 3.1: Eight Node Transformation

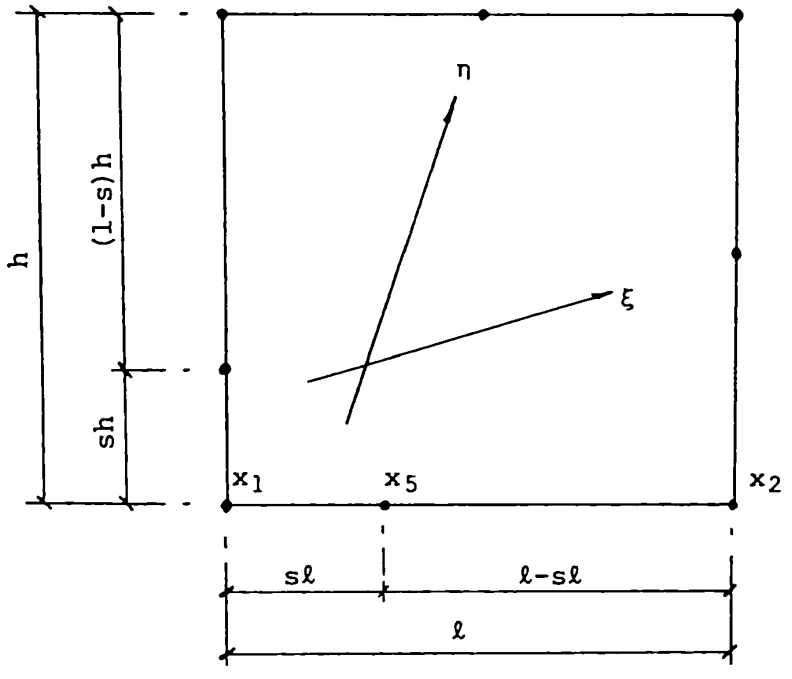

FIGURE 3.2: Location Shift for (x_5) to Induce Stress Singularity at (x_1)

CHAPTER 4

THEORY OF EIGHT-NODE TO SIX-NODE ELEMENT DEGENERATION

The most efficient procedure for generating finite element meshes employs small elements in regions of large stress gradients and larger elements where stress distributions are relatively uniform. With quadrilateral elements however, this condition is difficult to achieve, and it may require a relatively complex mesh. To accomodate large variations in a finite element mesh it is generally easier to use triangular elements. This is because dimensional changes can be readily accomodated in such a mesh configuration.

Very distorted quadrilateral elements, as shown in Figure 4.1, have been used by some authors [12]. However, even this approach might not provide the level of refinement desired in certain regions. Other authors [25] have combined the use of triangular and quadrilateral elements.

Instead of using two different ways to derive the quadrilateral and triangular elements, the degeneration technique reported in [26] has been used. This involves the

degeneration of a regular, eight-node, quadrilateral, isoparametric element into a triangular, six-node, isoparametric element. By the introduction of very straightforward modifications to the shape functions, six-node, triangular, isoparametric elements can be accomodated in a standard eight-node, quadrilateral finite element computer programme. Very flexible mesh configuration options are provided as a result, and it becomes considerably easier to construct a more computationally efficient mesh.

4.1 Element Degeneration

The basic procedure for degenerating an eight-node quadrilateral element into a six-node triangular element is simply to collapse the three nodes along one of the edges into a single node, Figure 4.2. This element would then be identified in the computer programme as a pseudo-eight-node element, where three nodes have identical coordinates. For this specific application, the node identification for the triangular element, Figure 4.3(b), would be:

3 : 5 : 14 : 14 : 4 : 10 : 14 : 9 ;

where the procedure is to identify the corner nodes first, starting with the lower,left-hand corner and proceeding in a

counter-clockwise order, followed by the mid-side nodes. For the standard quadrilateral element, Figure 4.3(a), the node identification would have been:

3 : 5 : 16 : 14 : 4 : 10 : 15 : 9 .

The analysis routine therefore regards the element as a quadrilateral, eight-node element with three coincident nodes.

The resultant element, however, may not provide the necessary spatial isotropy. As discussed by Bathe, lower order quadrilateral elements automatically yield a spatially isotropic triangular element through such a degeneration procedure. Typical elements would be of the four node type. However, for higher order elements, such as the eight-node quadrilateral, degeneration to a six-node triangular element destroys the geometrical invariance of the original element. In this situation, corrections must be applied to the element shape functions in order to restore the spatial isotropy.

For the element in Figure 4.4, it is desirable for the internal displacements, u and v, to vary identically for each nodal displacement, corner and mid-side. However, by simply collapsing one side into a single node, the resultant

shape functions are not compatible with the requirement that the element could be renumbered without any change to the displacement assumptions. The corrections, proposed by Bathe, allow the element to develop the necessary isotropy. The shape factors for the two elements, the standard eight-node element and the modified six-node element, are listed below. On comparison of the two arrays, it is of interest to note that the modified AN(3) value is a summation of the original AN(3), AN(4) and AN(7) factors, while the AN(1), AN(2) and AN(5) factors are modified to ensure isotropy. The development of the modified AN(3) shape factor is given in Appendix 1.

The modifications described were incorporated into the standard eight-node element coding, and triggered into use whenever a degenerated element was utilized.

Isoparametric element shape functions:

a) eight-node

$$AN(1) = 1/4(1-s)(1-t)(1+s+t)$$

$$AN(2) = -1/4(1+s)(1-t)(1-s+t)$$

$$AN(3) = -1/4(1+s)(1+t)(1-s-t)$$

$$AN(4) = -1/4(1-s)(1+t)(1+s-t)$$

$$AN(5) = 1/2(1-s^2)(1-t)$$

$$AN(6) = 1/2(1-t^2)(1+s)$$

$$AN(7) = 1/2(1-s^2)(1+t)$$

$$AN(8) = 1/2(1-t^2)(1-s)$$

b) six-node

$$AN(1) = -1/4(1-s)(1-t)(1+s+t) + Q$$

$$AN(2) = -1/4(1-s)(1-t)(1-s+t) + Q$$

$$AN(3) = 1/2(1+t) - 1/2(1-t^2)$$

$$AN(5) = 1/2(1-s^2)(1-t) - 2Q$$

$$AN(6) = 1/2(1-t^2)(1+s)$$

$$AN(8) = 1/2(1-t^2)(1-s)$$

$$Q = 1/8(1-s^2)(1-t^2)$$

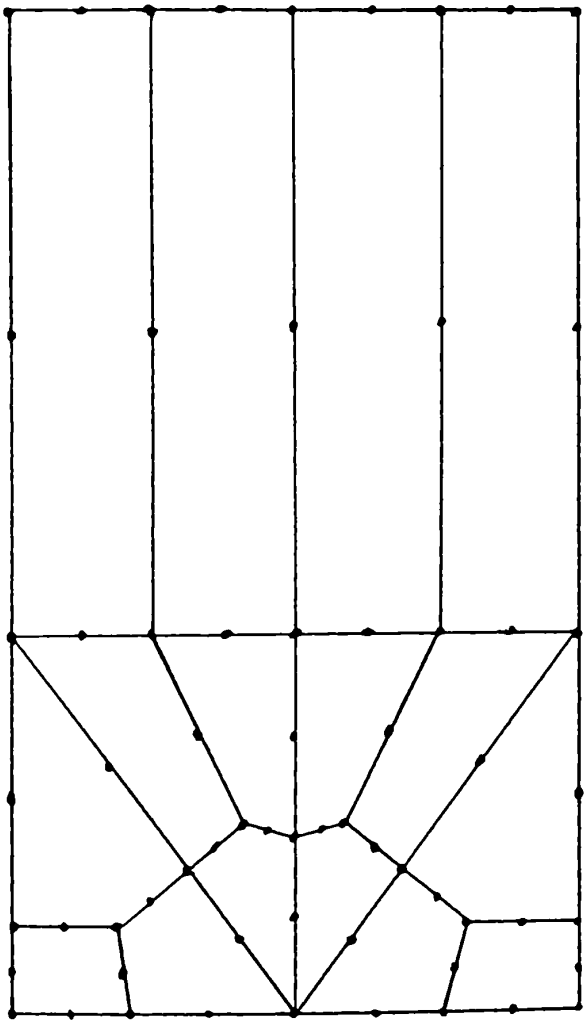

FIGURE 4.1: Distorted Quadrilateral Elements (Reference 12)

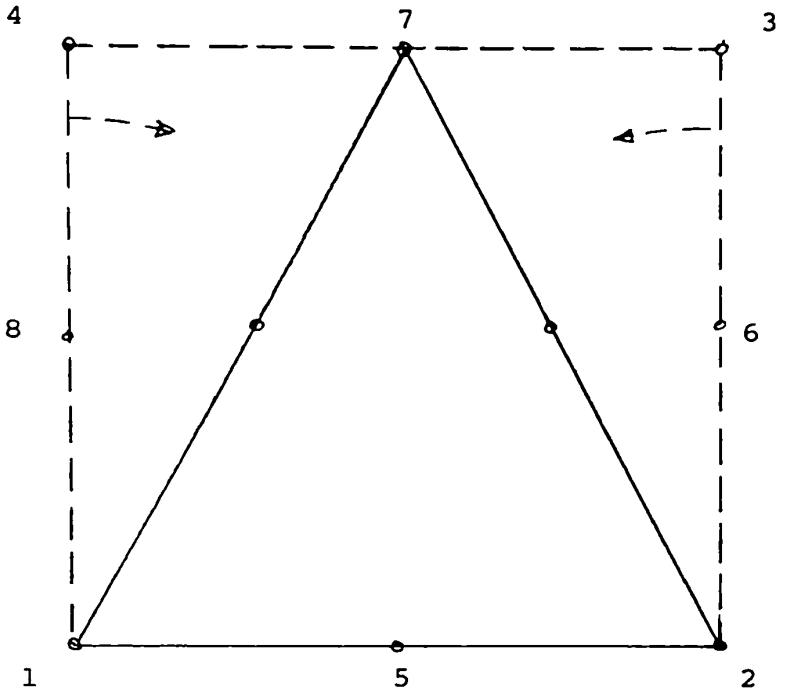

FIGURE 4.2: Collapsing Three Nodes into One Nodal Location

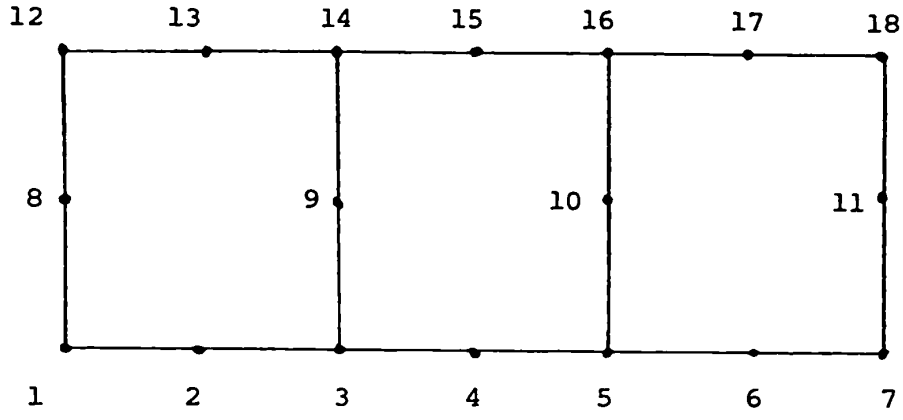

a) Standard Eight Node Quadrilateral Elements

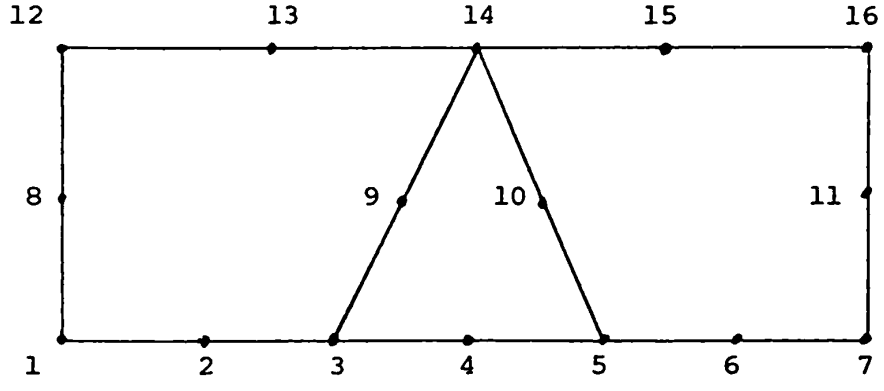

b) Eight Node and Degenerated Six Node Elements

FIGURE 4.3: Basic Eight Node and Degenerated Six Node Element Mesh Configurations

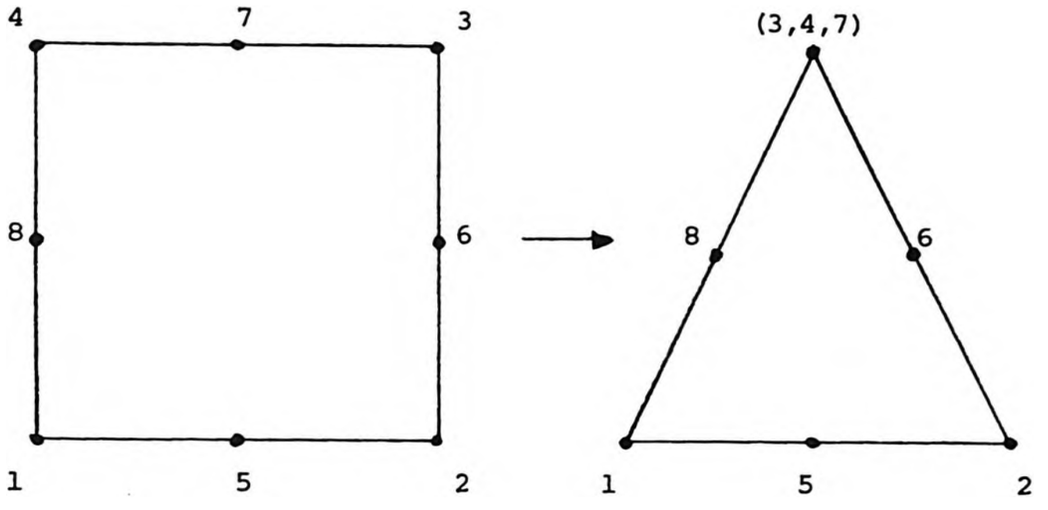

FIGURE 4.4: Typical Node Identification Theory

CHAPTER 5

APPLICATION OF FINITE ELEMENT METHOD TO FRACTURE METHODS

To verify the method developed in Chapters 3 and 4, and to ascertain its accuracy, several examples with known results have been investigated. Critical stress intensity factors are calculated for several crack length conditions in a centre-cracked strip (CCS) specimen and in a double-edge-notched strip (DENS) specimen, under tensile loads. These are then compared with results obtained by other researchers. Also, the problem of an orthotropic square plate with a centre crack is analysed, for several modular ratios, and compared with results available in the literature. It is readily apparent that the method described here is an accurate method for assessing crack characteristics.

5.1 Isotropic Rectangular Plates with a Central Crack, or with Symmetric Edge Cracks.

The two plane strain problems, for which there are considerable analytical results available in the literature, are shown in Figures 5.1 and 5.2. Recognizing the inherent

double symmetry of the specimens, only one quarter of the plate needs to be modelled, thus resulting in significant savings in computational costs. The section of the specimen to be investigated is therefore shown as the shaded area in Figures 5.1 and 5.2, along with the appropriate boundary conditions.

As the only difference between the CCS and the DENS problems is in the definition of the boundary conditions, the same mesh is used for both, as illustrated in Figure 5.3. This mesh utilizes a combination of standard and modified eight-node isoparametric elements, and six-node elements degenerated from the eight-node type. For the two elements that straddle the crack tip, the node-shift distortion, discussed in Chapter 3, is introduced. By moving the mid-side nodes on the three edges radiating from the crack tip to the quarter point positions nearest the tip, the required singularity condition is introduced. For the other elements in the crack region and for a distance from the crack that is sufficient to damp out major stress variations, standard elements are used. Then, in order to allow for mesh coarsening in the remainder of the specimen, a transition zone of six-node triangular elements is added. Finally, a zone of large, eight-node elements is used to represent the more regular sector of the specimen that is beyond the influence of the crack tip singularity.

For both the CCS and DENS problems, the energy release-rate approach is used to determine the stress intensity factor. In each case the stored strain energy is calculated for the body with the original crack, and then for three conditions of crack extension. The crack extension, in each case, represents an incremental growth of two percent of the original crack length. The difference between the strain energy values for each successive crack configuration, divided by the crack surface area increment, represents the strain energy released, ΔU, per unit of crack advance, Δa. In other words, this is the strain energy release rate: $(\Delta U/\Delta a)$. As discussed in Chapter 2, this can be represented as:

$$G_I = -\Delta u/\Delta a \qquad (5.1.1)$$

The calculated energy release rate is then used to determine the stress intensity factor for each configuration, according to Equation (2.1.8.b), which takes the following form for computation of K_I under plane strain conditions:

$$K_I = (EG_I/(1-\nu^2))^{1/2}$$
$$= [(E/(1-\nu^2))(-\Delta u/\Delta a)] \qquad (5.1.2)$$

The results of the CCS and DENS investigations are

given in Tables 5.1 and 5.2 respectively. By analyzing each specimen for four crack configurations, the consistency of the method is established and some indications of the relationship between crack length/specimen width ratio and stress intensity factor are provided. The nearly exact K_I values, defined by Mirza and Olson [13] and based on the original work of Bowie [27], and Bowie and Neal [28], are also provided, for comparison purposes. It can be observed that the finite element technique in this report provides a very accurate approach to the linear elastic, isotropic cracked body problem. Furthermore, there is only slight divergence from the exact data with increasing crack length, as expected. Errors of less than 1 percent for the CCS, and approximately 2 percent for the DENS are achieved, which are excellent considering the coarseness of the finite element mesh. More accurate results can be expected with further mesh refinement and smaller crack advance increments.

5.2 Orthotropic Square Plate with a Central Crack

The plane stress, orthotropic square plate with a central crack is shown in Figure 5.4. As for the investigations of the isotropic specimens in section 5.1, the double symmetry of the problem again requires only one quarter of the plate to be analysed. The finite element configuration for this specimen, along with the appropriate

boundary conditions, is indicated in Figure 5.5.

As before, a combination of standard and modified eight-node elements and degenerated six-node elements is used to model the cracked plate. Again, the strain energy release-rate method is adopted. However, owing to the anisotropy of the body, a slightly different strain energy release-rate/stress intensity factor relationship is required.

In the case of a crack propagating in its own plane, in an orthotropic body, the relationship between G and K is given by [2]:

$$G_I = \pi K_I^2 (2E_x E_y)^{-\frac{1}{2}} [(E_x/E_y)^{\frac{1}{2}} + (2(-\nu_{yx}/E_x) + (1/\mu_{xy}))/(2/E_x)] \quad (5.2.1)$$

where E_x and E_y are the principal elastic moduli, μ_{xy} is the shear modulus in the x-y plane, and ν_{yx} is Poisson's ratio for strain in y due to stress in x direction.

In describing results from the analysis, the approach due to Bowie and Freese [29] is employed. In their paper, they define two factors, β_1 and β_2, that characterize the response of a cracked orthotropic plate. These factors are defined such that:

$$\beta_1\beta_2 = (E_x/E_y)^{1/2} \qquad (5.2.2)$$

and

$$\beta_1+\beta_2 = \sqrt{2}((E_x/E_y)^{1/2}+(E_x/2\mu_{xy})-\nu_{yx})^{1/2} \qquad (5.2.3)$$

For purposes of this study, the β_1 factor is maintained as unity, while β_2 is assumed to vary. Also, the value of the shear modulus is kept as unity. The values of ν and β_2 are then selected such that Equation (5.2.3) is satisfied. A summary of the properties chosen is given in Table 5.3

The analysis involves calculating the strain energy release rate for a given crack advance, according to Equation (5.1.1) and then determining the stress intensity factor from Equation (5.2.1). Table 5.4 summarizes the results for the five different values of β_2 selected. The results of Bowie and Freese, for similar conditions, are also provided, for comparison purposes. From this comparison, it can be observed that there is very good agreement between the results of the present study and those of Bowie and Freese [29]. Errors range from 1.46 percent to 7.27 percent, which is very good considering the coarseness of the finite element mesh. Again, more accurate results can be achieved by using a more refined mesh.

2a	Δa	ΔU (1/4)	G_I	K_I	$K_I/\sigma\sqrt{a}$	Error (%)
10.0						
	0.2	1.020658	20.4132	4.7363	2.107	0.07
10.2						
	0.2	1.058078	21.1616	4.8223	2.1249	0.74
10.4						
	0.2	1.097229	21.9446	4.9107	2.1432	1.61
10.6						
Exact $K_I/\sigma\sqrt{a}$: ref [13] =					2.1092	

Table 5.1: Stress intensity factors from the finite element analysis of the centre-cracked specimen (Figure 5.1)

2a	Δa	ΔU (1/4)	G_I	K_I	$K_I/\sigma\sqrt{a}$	Error (%)
10.0						
	0.2	0.98922	19.7844	4.6627	2.0749	2.99
10.2						
	0.2	1.01787	20.3574	4.7298	2.0842	2.55
10.4						
	0.2	1.04762	20.9524	4.7984	2.0942	2.09
10.6						
Exact $K/\sigma\sqrt{a}$: ref [13] =					2.1388	

Table 5.2: Stress intensity factors from the finite element analysis of the double-edge-notched specimen (Figure 5.2).

$\beta_2^2 = E_x / E_y$	E_x	$E_y = E_x / \beta_2^2$	μ_{xy}	ν_{yx}
0.3	1.5	5.0	1.0	0.1
0.7	2.1667	3.09523	1.0	0.2333
1.0	2.6667	2.6667	1.0	0.3333
1.5	3.1667	2.1111	1.0	0.3333
4.5	6.1667	1.3704	1.0	0.3333

Table 5.3: Material properties used for the determination of the stress intensity factor for an orthotropic square plate with a centre crack.

$\beta_2^2 = E_x/E_y$	$K_I/\sigma\sqrt{a}$	Exact $K_I/\sigma\sqrt{a}$ ref.[29]	Error (%)
0.3	1.39	1.37	1.46
0.7	1.23	1.26	2.44
1.0	1.17	1.22	4.27
1.5	1.10	1.18	7.27
4.5	1.07	1.12	4.67

Table 5.4: Stress intensity factors from the finite element analysis of the square orthotropic plate with a centre crack (Figure 5.4)

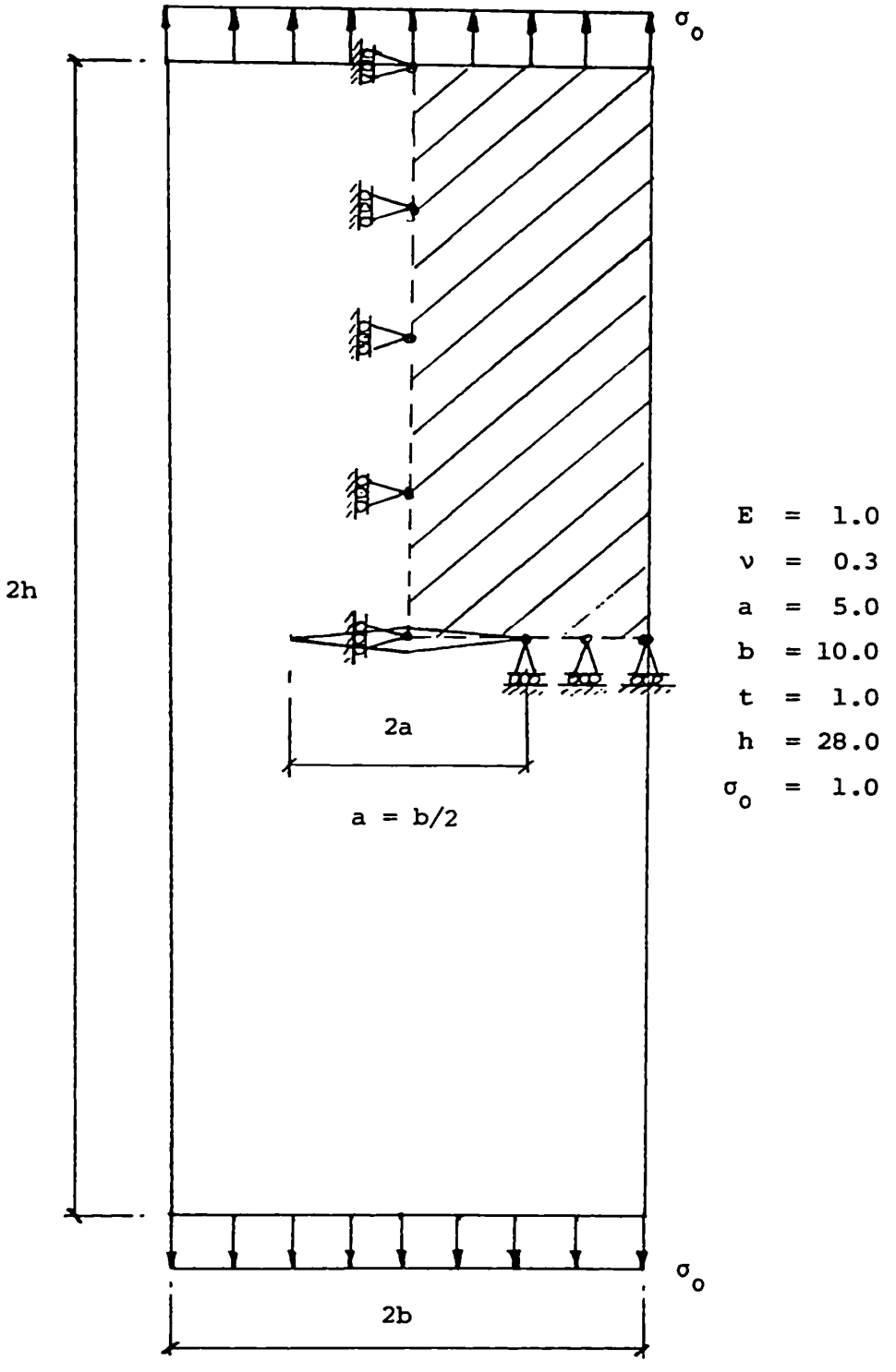

FIGURE 5.1: Rectangular Plate with a Central Crack

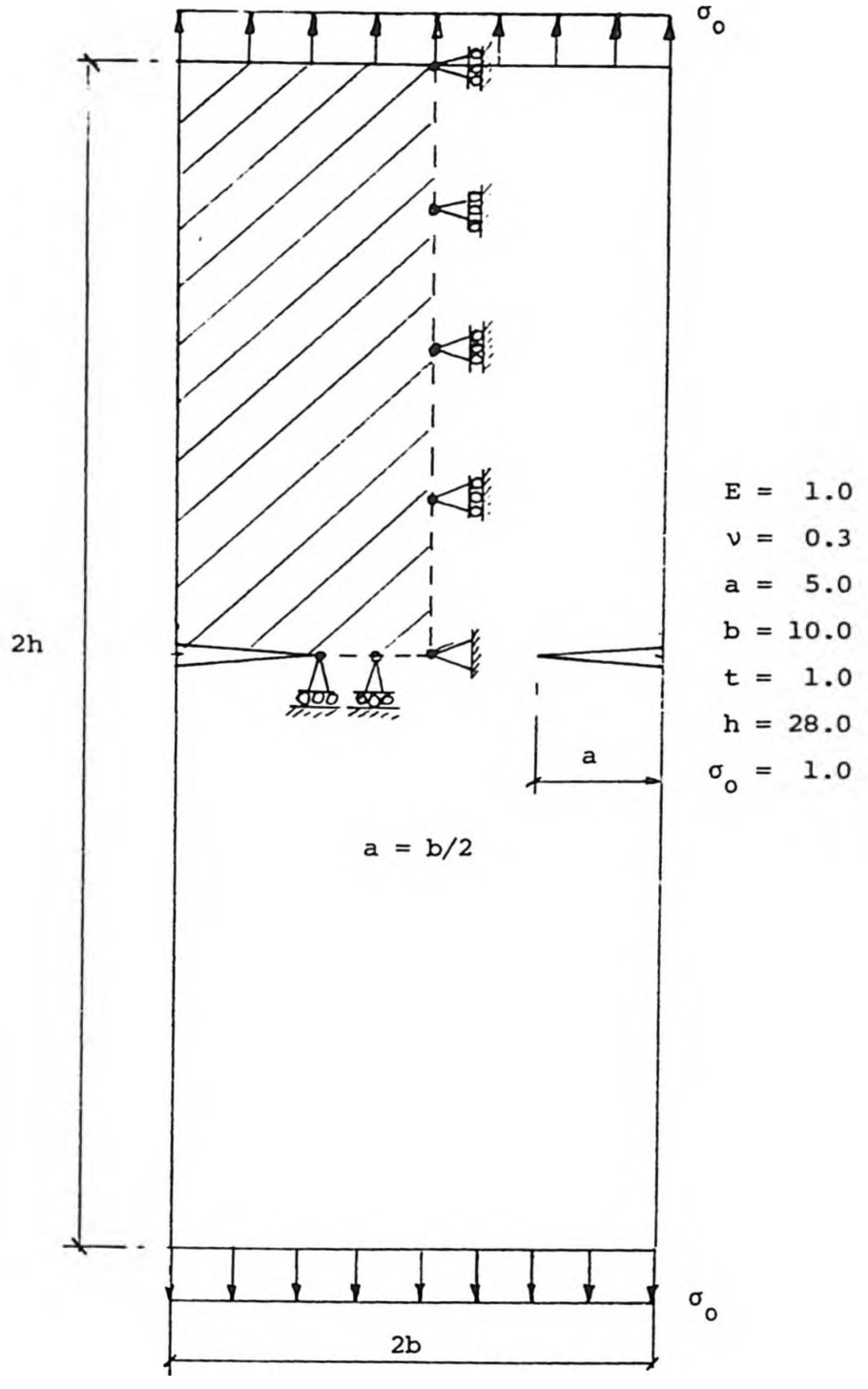

FIGURE 5.2: Rectangular Plate with Symmetric Edge Cracks

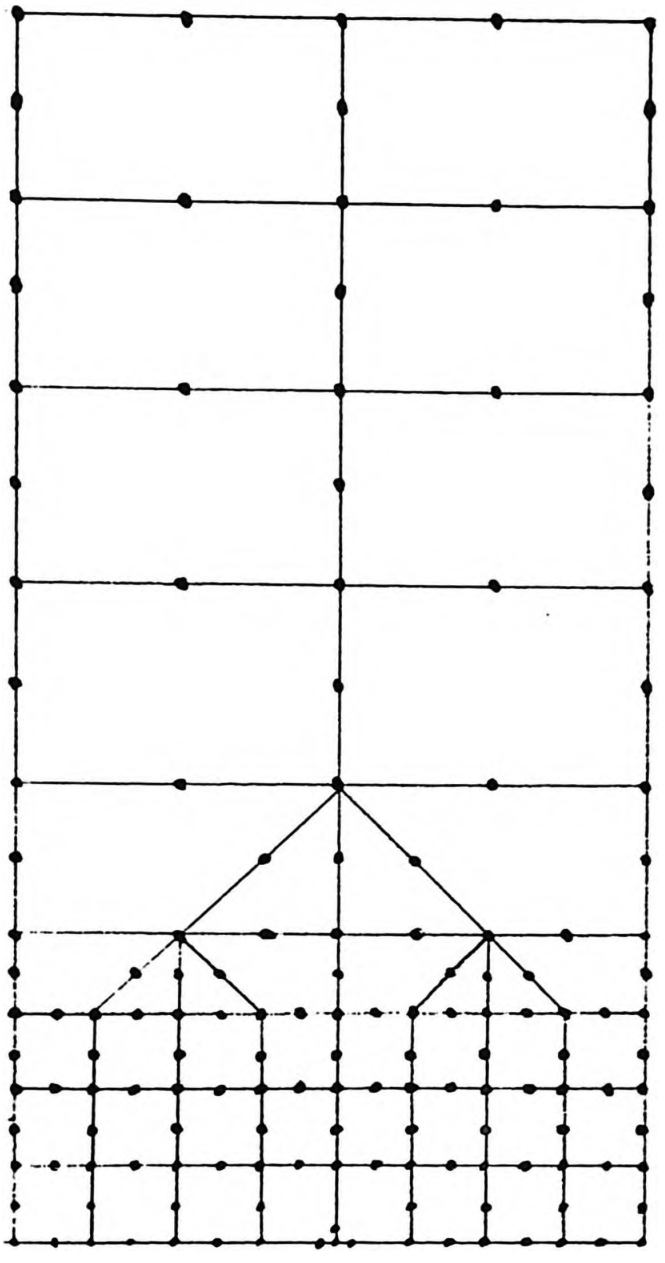

FIGURE 5.3: Finite Element Mesh for Rectangular Plate with Central Crack, or with Symmetric Edge Cracks

σ_o = 1.0
h/b = 1.0
a/b = 0.4
a = 1.2
b = 3.0
h = 3.0

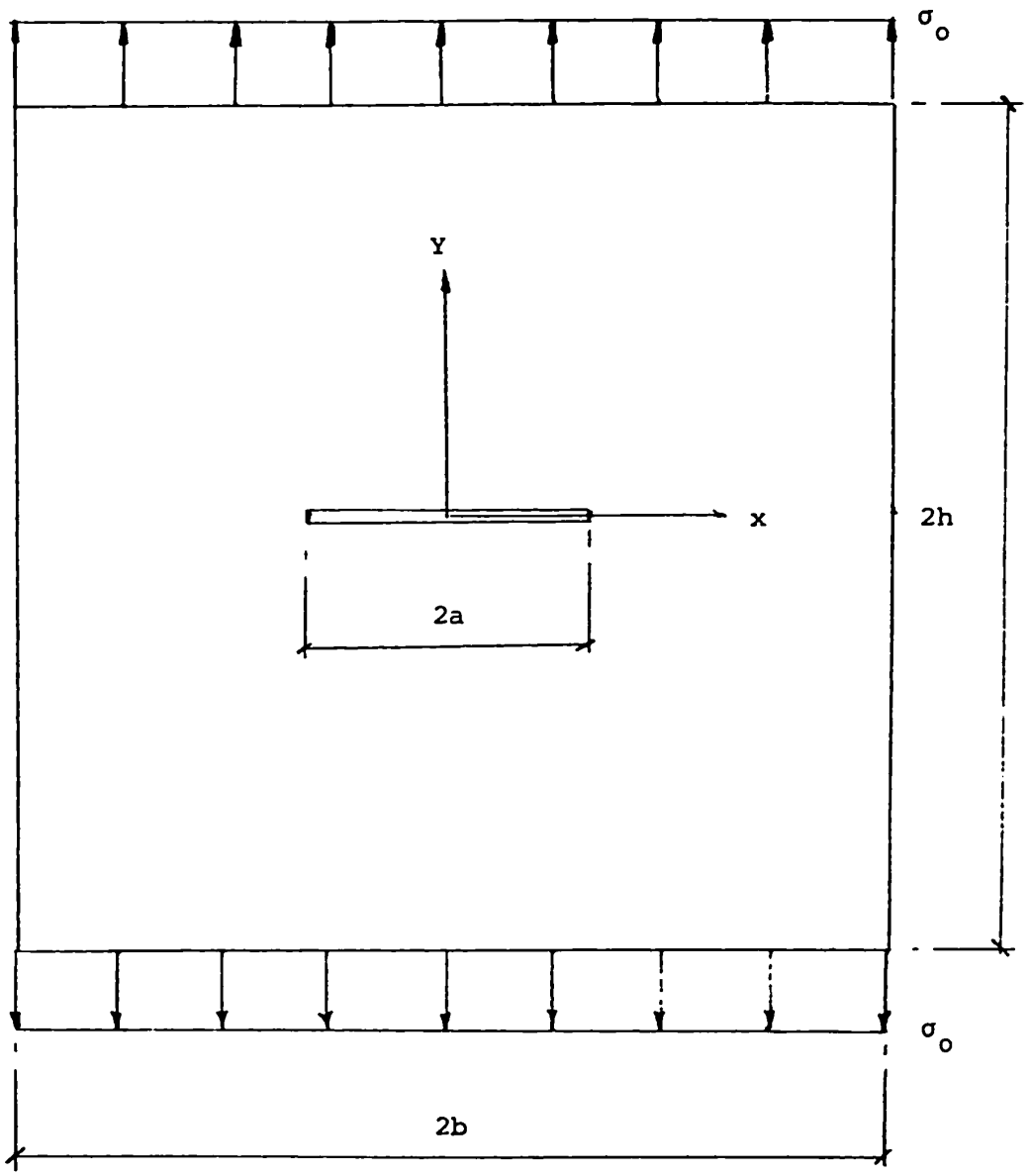

FIGURE 5.4: Orthotropic Square Plate with a Central Crack

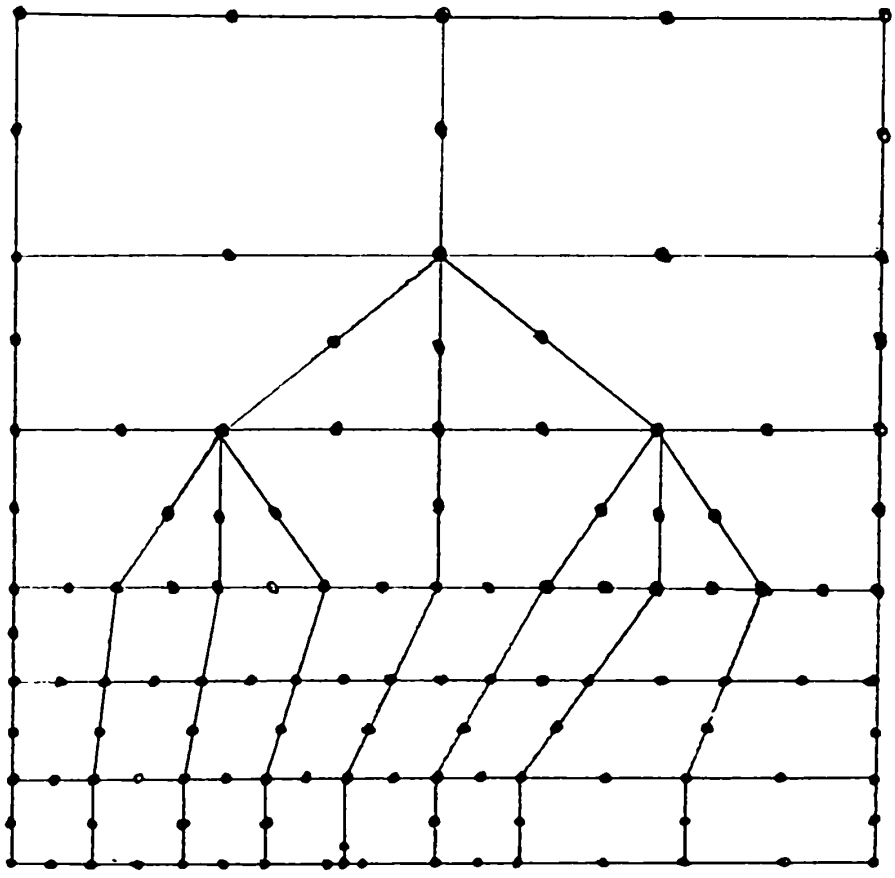

FIGURE 5.5: Finite Element Mesh for Orthotropic Square Plate with Central Crack

CHAPTER 6

EXTENSION OF FINITE ELEMENT METHOD TO CRACKED BODY PROBLEMS

As mentioned in section 2.1, the basic purpose of fracture mechanics is to provide a correlation between experimental data and actual service conditions, through quantitative relationships between applied stress, discontinuity size and material toughness. Such a relationship would make it possible to determine the condition of stress intensity factor for any set of geometric discontinuity and applied stress. Material adequacy could then be established by ensuring that the critical stress intensity factor for the selected material exceeds this computed factor for the application. In practice, this would result in the prediction of critical defect sizes for the anticipated stress conditions for a specific material, or conversely, the allowable stress that could be applied to a specific material with inherent discontinuities. In either case, fracture mechanics analysis would allow the establishment of the criteria for material selection and inspection.

The basic applicability and accuracy of the

particular finite element approach presented earlier were investigated for classical crack configurations. It is necessary however, to develop confidence in the use of the approach for more general geometric configurations, and for use with real materials. Such confidence can only be established by modelling specific cracked bodies for which experimental results are available. The results from both the analysis and the experiments can then be compared and assessed.

To this end, the standard single-edge-notch, three-point-bend (SENB-3) specimen is modelled analytically, and the results compared with experimental data for high-strength steels. The results of this investigation clearly define the limitations and practical uses of the finite element approach presented.

6.1 The Single-Edge-Notch, Three-Point-Bend (SENB-3) Specimen

The SENB-3 test, or bend bar test, is one of the most frequently used procedures for the experimental determination of the fracture toughness of metallic materials. The basic methodology of the procedure is contained in the ASTM E-399 specification [30], and discussed in detail in Rolfe's introductory text on fracture

mechanics [4]. The compact tension specimen (CTS) test, also covered by E-399, is the other most frequently used procedure. It is however, owing to its geometry, slightly more difficult to model by finite elements.

The principal limitation of the test is that it is only valid for materials that exhibit predominantly plane-strain behaviour. This limitation is primarily a result of the difficulty encountered in accommodating the significant plastic zone associated with plane stress behaviour. Consequently, the procedure is generally limited to relatively high strength steels, thick-section steel specimens, investigations of steels at very low temperatures, or non-ferrous materials that exhibit little crack zone plasticity, or brittleness. However, for the purpose of this present study, the limitations of the E-399 test procedure reflect the basic material assumptions of the finite element model and are thus of significant benefit. Any other type of material behaviour would probably necessitate the use of a three-dimensional finite element analysis, with inherent capabilities for modelling elastic-plastic behaviour.

While it is unnecessary to discuss the test procedures, some basic aspects are of interest at this time. The primary procedure is to develop a history of load versus

displacement for the specimen. The configuration is described in Figure 6.1. Then, on the resulting curve, such as that illustrated in Figure 6.2, a second line is drawn from the origin at a 5% offset to the tangent to the initial straight line portion of the trace. The point of intersection with the trace is given the load designation P_5. The load P_Q is then defined as follows: if the load at every point on the record which precedes P_5 is lower than P_5 then P_Q is P_5. If, however, there is a maximum load preceding P_5 which exceeds it, then this maximum load is P_Q. The ratio of Pmax /P_Q is calculated next, where Pmax is the maximum load that the specimen was able to sustain. If the ratio does not exceed 1.10, the following procedure is used to calculate K_Q:

$$K_Q = P_Q S/(BW)^{3/2} f(a/W) \qquad (6.1.1)$$

where B is the specimen thickness, S is the span length, W is the depth of specimen, a is the crack length, f(a/W) is a function of a/W.

$$f(a/W) = (2.9(a/W)^{1/2} - 4.6(a/W)^{3/2} + 21.8(a/W)^{5/2} - 37.6(a/W)^{7/2} + 38.7(a/W)^{9/2})$$

If the ratio exceeds 1.10, then the test is not valid for K_{IC} determination, since it is possible that K_Q

bears no relation to K_{IC}.

The next step is to calculate:

$$2.5(K_Q/\sigma_{ys}) \qquad (6.1.2)$$

where σ_{ys} = yield strength in tension

If both the specimen thickness (B) and crack length (a) are greater than the value of (6.1.2), then K_Q is K_{IC}. As discussed in Section 2.1, this value can then be assumed to represent a basic property of the material under study, and can be used to assess its susceptibility to unstable crack propagation in any other structural configuration, in a similar environment.

6.2 Finite Element Model of SENB-3 Specimen

The basic structural analogy of the specimen is illustrated in Figure 6.3. Due to symmetry, only one half of the specimen need be modelled, and this is illustrated as the shaded area in Figure 6.3, along with the appropriate boundary conditions. As for the problems in Chapter 5, a combination of standard and modified eight-node isoparametric elements and degenerated six-node elements is used to model the specimen. The mesh is illustrated in

Figure 6.4. Again, the energy release-rate approach is employed, and the strain energy release-rates computed for four crack extensions. The stress intensity factors are then computed, using Equation (5.1.2).

The results of the investigation are presented in Table 6.1. These are then compared with the results of an E-399 investigation on the fracture characteristics of an 18Ni-Maraging Steel (250 Grade) [31], Table 6.2. In order to properly compare these data sets, the stress intensity factors from the finite element analysis are normalized by the applied stress and $\sqrt{a}$, while the critical stress intensity factors for the 18Ni-250 steel are normalized by a factor of the applied load, P_Q. This value is calculated using Equation (6.1.1).

For the finite element data the average normalized value is:

$$K_I(ave.)/\sigma\sqrt{a} = 14.697 \qquad (6.2.1)$$

For the experimental data, the normalized values, based on the averages of the various orientations, is:

$$K_{Ic}/p\sqrt{a} = 15.075 \qquad (6.2.2)$$

where $p = P_Q/2$ (the factor of 1/2 being used to ensure equivalence with the finite element solution).

From the above, the considerable accuracy of the finite element approach is clearly established. For materials which exhibit primarily plane strain, or brittle, behaviour in the presence of an internal discontinuity, the method therefore becomes a reasonable predictor of tolerable strength.

6.3 Discussion of the Results

In evaluating the use and reliability of the finite element method in fracture mechanics problems, it is important to note the essential differences between Equations (6.2.1) and (6.2.2). In the case of the former, the finite element method is used to estimate the stress intensity factor resulting from the presence of a crack-like discontinuity. It is thus, primarily, a function of geometry and applied stress, except for the fact that material deformation is assumed to be one of plane-strain. For Equation (6.2.2) however, the purpose is to calculate the critical stress intensity factor for a particular material of interest. It is therefore a basic, inherent characteristic of the material.

Consequently, the finite element method should provide a lower bound for the fracture behaviour of a given material. In other words, the fracture toughness (K_{IC}) of most metallic materials is above the plane-strain threshold value. Thus, this limit should only be approached as materials start to approximate this type of behaviour.

In practice therefore, once the stress intensity factor for any given geometric configuration has been computed, it is only necessary to select a material that exhibits a K_{IC} property above this level.

For the particular material under study, the 18Ni-Maraging steel, the proximity of the fracture toughness characteristic to the computed plane strain stress intensity factor suggests that there is negligible plastic deformation at the crack tip for the environment of the test, and that the deformation was essentially one of plane-strain. The finite element programme could be used therefore, to investigate any proposed configuration, and provided that the calculated stress intensity factor was less than the experimentally determined K_{IC}, service should be acceptable.

For other materials, particularly those that exhibit reasonable plastic behaviour at the crack tip, care would have to be exercised. While the finite element method would

still provide a safe lower bound, the margin of safety introduced may be excessive. As a result, cost effectiveness may be less than satisfactory. Similarly, significant reductions in thickness may reduce some of the constraint that induced plane strain behaviour in the test specimen. Therefore, lighter sections may also be evaluated in an overly conservative manner by direct application of the finite element procedure. For these reasons, the finite element approach of this study is most cost effective when applied to materials that can be expected to exhibit plane strain behaviour in the proposed application environment.

a (in^2)	Δa (in^2)	ΔU (1/2) (in.-kips)	G_I (in.-ksi.)	K_I (ksi $\sqrt{in.}$)	$K_I/\sigma\sqrt{a}$
0.999					
	0.001	3.1609 x 10	3.1609 x 10	14.223	14.227
1.000					
	0.001	3.4826 x 10	3.4826 x 10	14.929	14.925
1.001					
	0.001	3.4927 x 10	3.4927 x 10	14.951	14.939
1.002					

Table 6.1: Stress intensity factors from finite element analysis of the SENB-3 specimen (Figure 6.5).

Specimen	Orientation	K_{Ic}	P_Q: (6.1.1)
1	Surface-Transverse	59.0	
2	" "	61.0	
		Avg 60.0	7.960
3	Midplane-Transverse	69.1	9.167
4	Surface-Longitudinal	72.2	
5	" "	69.6	
		Avg 70.9	9.406
6	Midplane-Longitudinal	70.9	
7	" "	74.9	
		Avg 72.9	9.672

Specimens were selected from both the surface and midplane locations of the source billet. The transverse and longitudinal orientationrefers to the specimen, thus the notch would be perpendicular to this direction.

Table 6.2: Experimentally determined critical stress intensity values for an 18Ni-Maraging Steel (250 Grade).

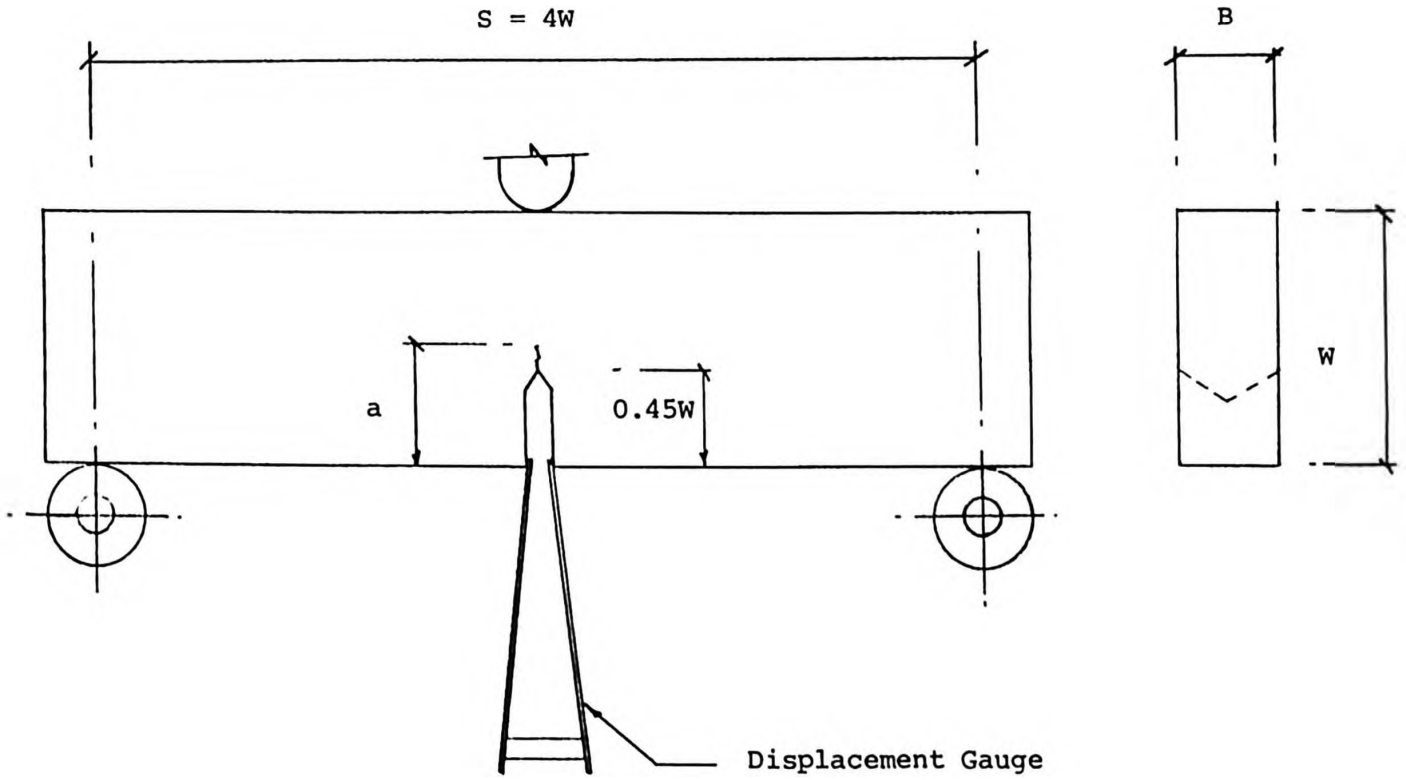

FIGURE 6.1: Standard Bend Bar Specimen Configuration

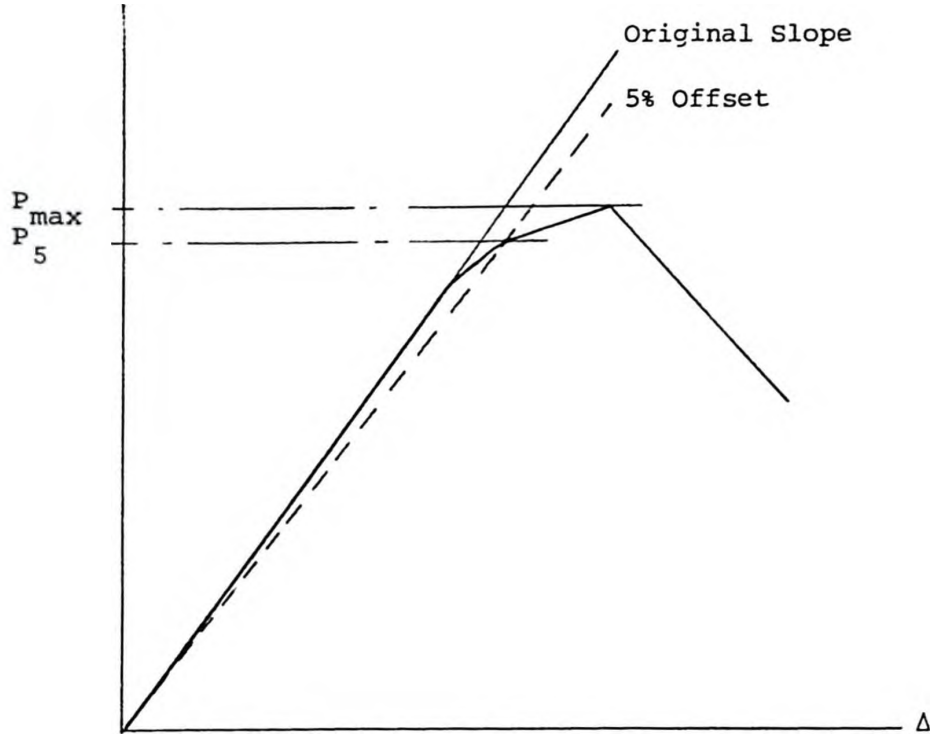

FIGURE 6.2: Typical P-Δ Curve for K_{IC} Determination

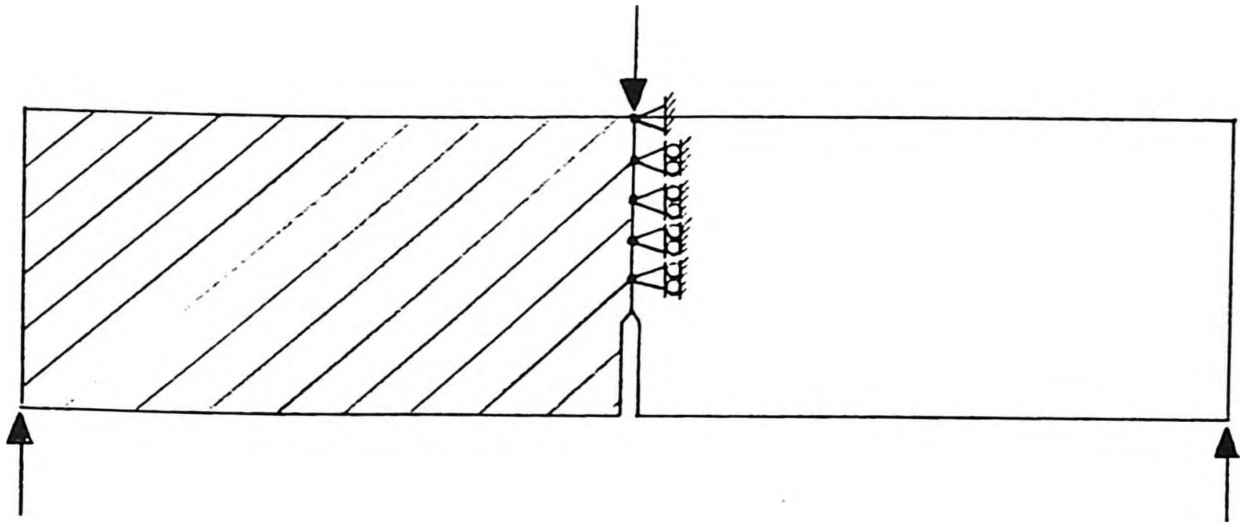

FIGURE 6.3: Structural Analogy of Bend Bar Specimen

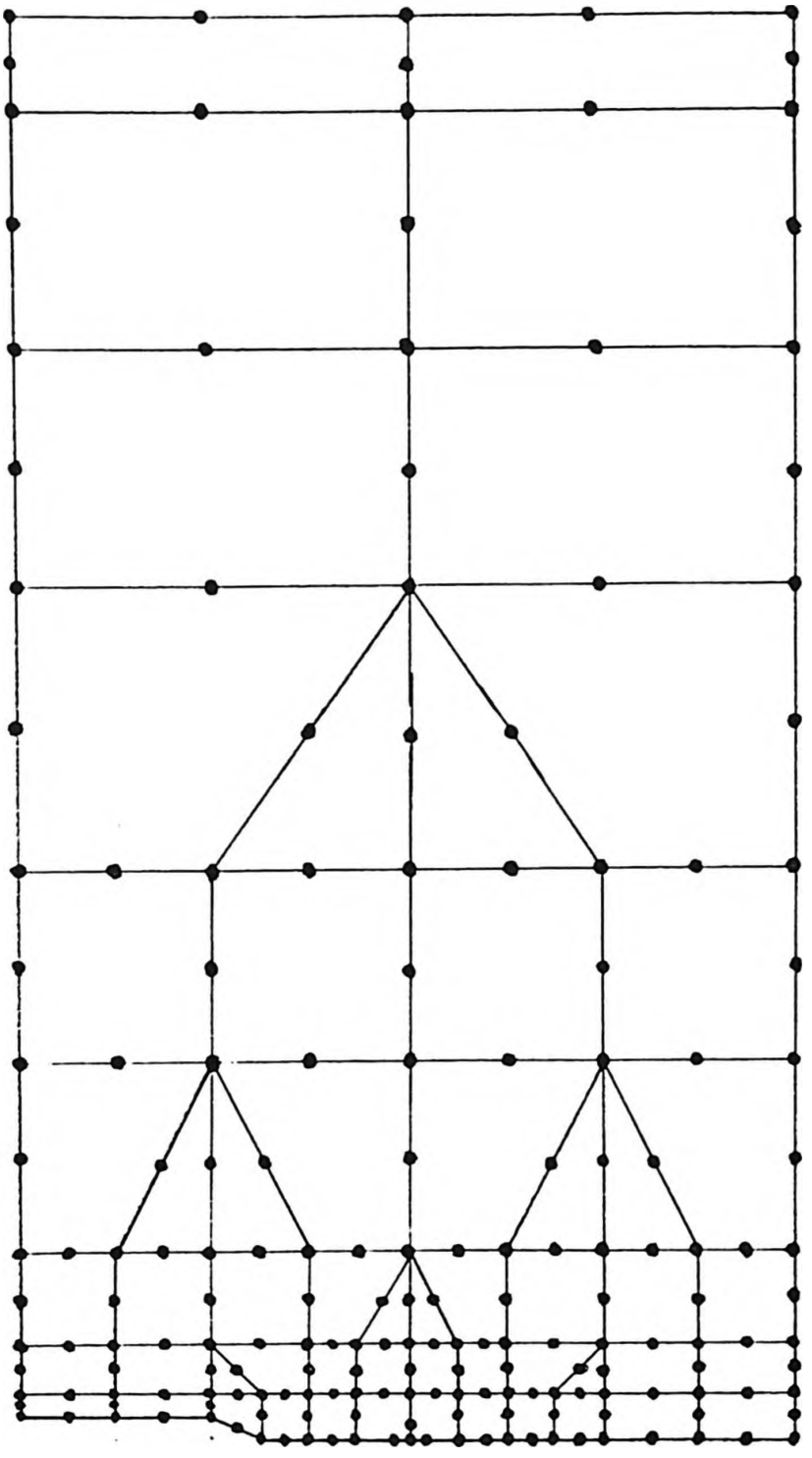

FIGURE 6.4: Finite Element Mesh for Bend Bar Specimen

CHAPTER 7

CONCLUSIONS AND RECOMMENDATIONS

It has been shown that, via a few minor modifications, a standard eight-node isoparametric finite element programme can be used to describe, accurately and economically, stress behaviour in the presence of a sharp, crack-like discontinuity in structural materials. For the cases of isotropic cracked strip specimens, and for an orthotropic cracked plate specimen, accurate results are achieved, using a coarse finite element mesh.

The principal modification, consisting of the shifting of the mid-side node on edges adjacent to the tip of the discontinuity, is shown to induce the required $1/\sqrt{r}$ stress singularity at the crack tip. This singularity condition occurs at the element corner node, when the mid-side nodes on the two adjacent sides are relocated to the quarter-point positions nearest the corner coincident with the crack tip.

In the investigation presented, only the quadrilateral elements are used in the crack-tip region, though it has been suggested [12] that degenerated

triangular elements, with relocated mid-side nodes, would improve the accuracy of the solution. Therefore, it is recommended that further work along these lines might prove beneficial in the development of a more refined and accurate finite element model.

The other significant modification incorporated in this analysis, though it has no direct effect on the fracture analysis, is the option to utilize a six-node element degenerated from a standard eight-node isoparametric element. This modification, which significantly enhances the flexibility of mesh configuration, can be easily implemented without any effect on neighbouring eight-node element regions. Certain interpolation function changes [26] are also incorporated, to ensure spatial isotropy within the degenerated element.

With the above modifications, and using relatively coarse mesh models, stress intensity factors for the isotropic, cracked strip specimens are determined to within 3 percent of the exact values. Slightly less accurate, but still satisfactory results are achieved for the analysis of the cracked orthotropic plate. In this case, results varying between 1.5 percent and 7.25 percent of the values reported in the literature are obtained. For most engineering applications, particularly for situations

concerning defects in structural materials, accuracies of this order are quite acceptable.

The finite element model presented in this report is also used for the analysis of a standard bend bar specimen [30], and the results compared to data obtained from actual experiments with such specimens. This analysis not only further defines the level of accuracy to be expected from the specific finite element approach, but also illustrates the practical use of the method in design and manufacture. The experimental data used, was developed from an investigation of 18Ni-Maraging steel (250 Grade), utilized in the construction of various jet fighter aircraft. The finite element solution, for the theoretical plane strain condition, lies within 2.5 percent of the experimental data. This extremely close result suggests almost complete plane-strain deformation for the material; an extremely undesirable feature for a structural component in such a high priority application. In actual fact, this material has been removed from service in such applications, and replaced by a steel that exhibits significantly better ductility in the actual operating conditions.

With respect to practical applications of the finite element approach in engineering design, it can be observed that this specific model can be used to predict accurately

the stress intensification behaviour around crack-like discontinuities in materials that exhibit essentially plane-strain behaviour. As a result, for any geometric configuration and applied stress condition, the stress intensity around a sharp discontinuity can be estimated. Material selection criteria, with respect to inherent notch ductility, will then depend on ensuring that the proposed material possesses a basic fracture toughness, K_{IC}, in excess of the analytically determined stress intensity factor. Conversely, for a given material, for which the fracture toughness has been determined, and crack configuration, the finite element method can be used to predict the safe operating stress.

In both these cases, fracture mechanics can be used either to set inspection criteria, or material selection criteria based on inspection capabilities; that is, based on a given material and applied stess, critical defect sizes can be estimated. Inspection criteria can then be introduced such that similar defects are detected, with a high degree of reliability. On the other hand, if the practical limitations of the non-destructive testing equipment are known, then materials can be selected such that, for the proposed applied stress, the critical defect size will be greater than the detectable defect.

However, the inherent limitations of the present approach are readily apparent, in that reliable results can only be expected for materials which exhibit essentially plane-strain behaviour. With considerable plastic deformation in the vacinity of the crack tip, very conservative predictions of stress intensity factors are developed. Consequently, while the use of the finite element approach will generally lead to safe design assumptions, cost effectiveness may be adversely affected to a significant degree.

Unfortunately, for most metallic materials, in engineering applications, plane-strain behaviour occurs infrequently, such as with very thick sections or at low temperatures. Generally, considerable plastic deformation accompanies crack propagation, and thus significantly varying deformation modes are encountered across the crack front and around the crack.

Therefore, it is recommended that further attention be given to the development of practical finite element analysis methods for crack problems in the non-plane-strain regime. In addition a more detailed investigation into the practical use of plane-strain analysis programmes for non-plane-strain problems is recommended. For many applications, particularly with respect to the use of high

strength low alloy (HSLA) steels in off-highway equipment, bridges, offshore structures and Arctic vessels, the operating environment may be such that otherwise ductile materials tend toward a plane-strain type of behaviour. In such cases, the analytical stress intensity factor obtained from the plane-strain finite element analysis may, with the proper application of qualitative engineering judgement, be used to adequately predict acceptable performance criteria. With the growing importance of such applications, further research into the practical application of the finite element method is strongly recommended and clearly warranted.

Appendix 1

Derivation of AN(3) Shape Factor for Degenerated Six-Node Isoparametric Element.

AN(3) modified = (AN(3)+AN(4)+ AN(7)) original

$$= -\tfrac{1}{4}(1+s)(1+t)(1-s-t) - \tfrac{1}{4}(1-s)(1+t)(1+s-t) + \tfrac{1}{2}(1-s^2)(1+t)$$

$$= -\tfrac{1}{4}(1+s)(1+t)(1-t) + \tfrac{1}{4}s(1+s)(1+t) - \tfrac{1}{4}(1-s)(1+t)(1-t) - \tfrac{1}{4}s(1-s)(1+t) + \tfrac{1}{2}(1-s^2)(1+t)$$

$$= -\tfrac{1}{4}(1+s)(1-t^2) - \tfrac{1}{4}(1-s)(1-t^2) + \tfrac{1}{4}s(1+s)(1+t) - \tfrac{1}{4}s(1-s)(1+t) + \tfrac{1}{2}(1-s^2)(1+t)$$

$$= -\tfrac{1}{4}(1-t^2)\left[1+s+1-s\right] + \tfrac{1}{4}(1+t)\left[s+s^2-s+s^2+2-2s^2\right]$$

$$= \tfrac{1}{2}(1+t) - \tfrac{1}{2}(1-t^2)$$

APPENDIX 2

PROGRAMME LISTINGS

```
RAM TST        73/173  TS TRACE                          FTN 4.8+577        83/1

      PROGRAM TST(INPUT,OUTPUT,TAPE5=INPUT,TAPE6=OUTPUT,TAPE1)
      DIMENSION LJ(16),X(8),Y(8),S(16,16),FL(16),U(16),V(3,16),D(3,3),
     1AN(8),ANS(8),ANT(8),A(35000),B(400),XX(200),YY(200),IX(400),
     2JX(400),CON(10),ICON(10),BB(400),XLOAD(400),CPLN(3,3)
      DIMENSION ICO(56,11)
      WRITE(6,1)
    3 READ(5,2) NPROB,IPS,IGR,MT,NS,THICK,GR
      IF(EOF(5).EQ.1.0) GO TO 999
      READ(5,4) NEL,NNOD,NVAR,NNODEL
      IF(IPS.EQ.0) WRITE(6,25)
      IF(IPS.EQ.1) WRITE(6,26)
      IF(IPS.EQ.2) WRITE(6,25)
      IF(IPS.EQ.3) WRITE(6,26)
      WRITE(6,27) MT,NS,IGR,THICK,GR
      NVEL=NVAR*NNODEL
      CALL LAYOUT(XX,YY,ICO,IX,JX,NEL,NNOD,NVAR,NMAT,NNET,NNODEL)
      CALL BANDWH(ICO,JX,LJ,NEL,NVAR,LBAND,NNODEL)
      NB3=LBAND+1
      NVA=NB3*NNET
      WRITE(6,5) NPROB,NNET,LBAND,NVA
      CALL PRESET(S,NVEL,NVEL)
      CALL PRESET(D,3,3)
      CALL PRESET(CPLN,3,3)
      CALL PSET(A,NVA)
      CALL PSET(B,NNET)
      CALL PSET(BB,NNET)
      CALL PSET(XLOAD,NNET)
      READ(5,6) E,ANU,NCON
      IF(IPS.GE.2) GO TO 500
      WRITE(6,7) E,ANU,NCON
      IF(IPS.EQ.0) GO TO 18
      E=E/(1.00-ANU*ANU)
      ANU=ANU/(1.00-ANU)
   18 D(1,1)=E/(1.00-ANU*ANU)
      D(1,2)=ANU*D(1,1)
      D(2,2)=D(1,1)
      D(2,1)=D(1,2)
      D(3,3)=E/(2.00*(1.00+ANU))
      GO TO 503
  500 READ(5,504) EY,ANUZY,GXY
      EX=E
      ANUYX=ANU
      XN=EX/EY
      ANUXY=ANUYX/XN
      WRITE(6,501) EX,ANUXY,EY,ANUYX,GXY,ANUZY
      IF(IPS.EQ.3) GO TO 502
      D(1,1)=EX/(1.00-XN*ANUXY**2)
      D(1,2)=D(1,1)*ANUXY
      D(2,1)=D(1,2)
      D(2,2)=D(1,1)/XN
      D(3,3)=GXY
      CPLN(1,1)=1.000/EX
      CPLN(1,2)=-XN*ANUXY/EX
      CPLN(2,1)=CPLN(1,2)
      CPLN(2,2)=XN/EX
      CPLN(3,3)=1.000/GXY
      GO TO 503
```

```
PROGRAM TST        73/173  TS TRACE                    FTN 4.8+577        83/12
      502 CONTINUE
          CPLN(1,1)=(1.00-(ANUYX**2)*EY/EX)/EX
          CPLN(1,2)=-ANUYX*(1.00+ANUZY)/EX
          CPLN(2,1)=CPLN(1,2)
          CPLN(2,2)=(1.00-ANUZY**2)/EY
          CPLN(3,3)=1.CC0/GXY
          DDD=EX/((1.CC+ANUZY)*(1.00-ANUZY-2.00*ANUYX*ANUYX/XN))
          D(1,1)=(1.00-ANUZY**2)*DDD
          D(1,2)=ANUYX*(1.00+ANUZY)*DDD/XN
          D(2,1)=D(1,2)
          D(2,2)=(1.00-ANUYX**2/XN)*DDD/XN
          D(3,3)=GXY
      503 CONTINUE
          IF(NCON.EQ.0) GO TO 13
          READ(5,14) (ICON(I),I=1,NCON)
          READ(5,15) (CON(I),I=1,NCON)
          WRITE(6,16) (ICON(I),I=1,NCON)
          WRITE(6,17) (CON(I),I=1,NCON)
       13 REWIND 1
          DO 8 IEL=1,NEL
          DO 9 I=1,NNODEL
          ICOO=ICO(IEL,I)
          X(I)=XX(ICOO)
        9 Y(I)=YY(ICOO)
          IS=ICO(IEL,NNODEL+1)
          IB=ICO(IEL,NNODEL+2)
          ITRI=ICO(IEL,NNODEL+3)
          CALL ISOPAR(X,Y,S,FL,V,D,AN,ANS,ANT,THICK,GR,IS,IGR,ITRI)
          CALL BONDRY(FL,X,Y,AN,ANS,ANT,THICK,IS,IB,IEL,ITRI)
          DO 10 J=1,NNODEL
          J1=(J-1)*NVAR
          J2=NVAR*(ICO(IEL,J)-1)
          DO 10 I=1,NVAR
       10 LJ(I+J1)=JX(J2+I)
          CALL SETUP(A,B,S,FL,NVEL,LJ,NVAR,LBAND)
          WRITE(1) (X(I),I=1,NNODEL),(Y(I),I=1,NNODEL),(LJ(I),I=1,NVEL),
         1(ITRI)
        8 CONTINUE
          IF(NCON.EQ.0) GO TO 11
          CALL PLACEZ(B,A,CON,ICON,NCON,NNET,LBAND)
       11 DET=1.E-8
          WRITE(6,101)
          DO 100 I=1,NNET
          XLOAD(I)=B(I)
          WRITE(6,102) I,B(I),XLOAD(I)
      100 CONTINUE
      101 FORMAT(/,7X,"I",17X,"B(I)",30X,"XLOAD(I)",//)
      102 FORMAT(5X,I5,5X,F25.14,5X,F25.14)
          CALL BAND(A,B,NNET,NB3,1,DET)
          IF(DET.LE.0.00) GO TO 998
          WRITE(6,12) DET
          CALL EXPAND(BB,NMAT,B,JX,NNOD,NVAR)
          WRITE(6,103)
          DO 104 I=1,NNET
          WRITE(6,105) I,B(I)
      104 CONTINUE
      103 FORMAT(/,7X,"I",7X,"B(I)",//)
```

```
GRAM TST        73/173  TS TRACE                              FTN 4.8+577        83/12

  105 FORMAT(5X,I5,5X,F25.14)
      SSE=0.0
      DO 120 I=1,NNET
  120 SSE=SSE+XLOAD(I)*B(I)*0.5
      WRITE(6,130) SSE
  130 FORMAT(//,5X,"STORED STRAIN ENERGY = ",F25.14,//)
      REWIND 1
      WRITE(6,24)
      DO 19 IEL=1,NEL
      READ(1)  (X(I),I=1,NNODEL),(Y(I),I=1,NNODEL),(LJ(I),I=1,NVEL),
     1(ITRI)
      DO 20 J=1,NVEL
      IKK=LJ(J)
      IF(IKK) 21,22,21
   22 U(J)=0.00
      GO TO 20
   21 U(J)=B(IKK)
   20 CONTINUE
      WRITE(6,23) IEL
      CALL SIGISO(X,Y,V,D,U,AN,ANS,ANT,MT,NS,ITRI)
   19 CONTINUE
      WRITE(6,996)
      GO TO 3
  998 WRITE(6,997) DET
      GO TO 3
  999 STOP
    1 FORMAT("1",10X,"**********  PLANE ELASTICITY EIGHT NODE ISOPARAMET
     1RIC ELEMENT  **********",///)
    2 FORMAT(5I5,2F10.0)
    4 FORMAT(4I5)
    5 FORMAT(/,5X,"PROBLEM NO.",I5,10X,"TOTAL UNKNOWNS",I5,//,5X,"BANDWI
     1DTH",I5,10X,"MATRIX SIZE",I8,/)
    6 FORMAT(2F15.0,I5)
    7 FORMAT(/,5X,"MODULUS OF ELASTICITY =",F15.1,10X,"POISSONS RATIO ="
     1,F8.4,//,5X,"NUMBER OF CONSTRAINTS =",I6,/)
   12 FORMAT(/,5X,"DETERMINANT IS =",E20.8,/)
   14 FORMAT(20I4)
   15 FORMAT(8F10.0)
   16 FORMAT(/,5X,"CONSTRAINTS ON DOF",8I10)
   17 FORMAT(/,5X,"CONSTR. VALUES ARE",8F10.4)
   23 FORMAT(/,5X,"******** STRESSES IN ELEMENT NUMBER",I5,"********")
   24 FORMAT(//,9X,"N",9X,"M",12X,"XX",12X,"YY",8X,"RADIUS",9X,"THETA",6
     1X,"SIGMA-XX",6X,"SIGMA-YY",6X,"SIGMA-XY",//)
   25 FORMAT(//,35X,"*****  PLANE STRESS CASE  *****",//)
   26 FORMAT(//,35X,"*****  PLANE STRAIN CASE  *****",//)
   27 FORMAT(//,5X,"NUMBER OF STRESS CALCULATIONS IN T-DIRECTION = MT ="
     1,I5,//,5X,"NUMBER OF STRESS CALCULATIONS IN S-DIRECTION = NS =",I5
     2,//,5X,"IGR = ",I5,15X,"THICKNESS = ",F10.5,15X,"DENSITY = ",F10.5
     3,//)
  996 FORMAT(//,5X,"**********  END  **********",/)
  997 FORMAT(/,5X,"MATRIX IS NOT POSITIVE DEFINITE",5X,"DET =",E20.8)
  501 FORMAT(/,5X,"MODULUS OF ELASTICITY (X) = ",F15.1,10X,"POISSONS RAT
     1IO (XY) = ",F8.4,/,5X,"MODULUS OF ELASTICITY (Y) = ",F15.1,10X,"PO
     2ISSONS RATIO (YX) = ",F8.4,/,5X,"SHEAR MODULUS (XY) = ",F15.2,10X,
     3"POISSONS RATIO (ZY) = ",F8.4,//)
  504 FORMAT(3F15.0)
      END
```

```
TINE LAYOUT      73/173  TS TRACE                           FTN 4.3+577          83/11

      SUBROUTINE LAYOUT(X,Y,ICO,IX,JX,NE,NN,NVAR,NMAT,NDEG,NNODEL)
      DIMENSION X(1),Y(1),ICO(NE,1),IX(1),JX(1)
      NNN=NNODEL+3
      WRITE(6,41) NE,NN,NVAR,NNODEL
      WRITE(6,42)
      DO 10 I=1,NN
      I2=NVAR*I
      I1=I2-NVAR+1
      READ(5,43) X(I),Y(I),(IX(J),J=I1,I2)
      WRITE(6,44) I,X(I),Y(I),(IX(J),J=I1,I2)
   10 CONTINUE
      WRITE(6,47)
      DO 11 I=1,NE
      READ(5,45) (ICO(I,J),J=1,NNN)
   11 WRITE(6,46) I,(ICO(I,J),J=1,NNN)
      NMAT=NVAR*NN
      NDEG=0
      DO 12 I=1,NMAT
      IF(IX(I)) 1,2,3
    3 IF(IX(I)-1) 80,80,81
   81 NDEG=NDEG+IX(I)
      GO TO 82
   80 NDEG=NDEG+1
   82 JX(I)=NDEG
      GO TO 12
    1 NDEG=NDEG+IX(I)+1
      JX(I)=NDEG
      GO TO 12
    2 JX(I)=0
   12 CONTINUE
   41 FORMAT(//,4X,"TOTAL NO. OF ELEMENTS ",I5,5X,"NO.OF NODES",I5,5X,
     1"VARIABLES PER NODE",I5,3X,"NO. OF NODES PER ELEM.",I5,/)
   42 FORMAT(/,4X,"NODE",6X," X-CORD",6X,"Y-CORD",7X," U",3X,"V",/)
   43 FORMAT(2F10.0,6I3)
   44 FORMAT(1X,I5,5X,F10.6,2X,F10.6,5X,6I4)
   45 FORMAT(16I3)
   46 FORMAT(5X,I5,6X,8I4,2X,3I5)
   47 FORMAT(/,5X,"ELEMENT",9X,"N O D E   N U M B E R S",8X,"IS",3X,"I3",
     15X,"ITRI",//)
      RETURN
      END

        INPCI.       INPCR.       OUTCI.       OUTCR.       TAPE5#       TAPE6#
E:LS--

               175B          .2              206B            .3             153B
 ID            116B          .12       D     211B            .41      F     226B
  F            252B          .44       F     255B            .45      F     261B
  F            266B          .80             165B            .81            157B
```

```
      SUBROUTINE SETUP(A,B,S,FL,NVEL,LJ,NVAR,LBAND)
      DIMENSION A(1),B(1),S(NVEL,1),FL(1),LJ(1)
      DO 12 I=1,NVEL
      LJR=LJ(I)
      IF(LJR.EQ.0) GO TO 12
      B(LJR)=B(LJR)+FL(I)
      DO 11 J=1,NVEL
      LJC=LJ(J)
      IF(LJC.EQ.0)  GO TO 11
      IF(LJR-LJC) 9,10,10
   10 K=(LJC-1)*LBAND+LJR
      GO TO 13
    9 K=(LJR-1)*LBAND+LJC
   13 A(K)=A(K)+S(I,J)
   11 CONTINUE
   12 CONTINUE
      RETURN
      END
```

ELS--

```
         42B            .10             34B           .11     D       57B
         47B

 R A      0B             1               B       R A      0B           1
 R A      0B             1               I       I      101B
 I      105B                             K       I      102B
 I A      0B             .               LJ      I A      0B           1
 I      103B                             LJR     I      104B
 I A      0B                             NVEL    I A      0B
 R A      0B          VAR-DIM            SETUP   -       72B  ENTRY
```

M-UNIT LENGTH 19 SYMBOLS

ORAGE USED .186 SECONDS

```
TINE BANDWH     73/173  TS TRACE                          FTN 4.8+577          83/12

      SUBROUTINE BANDWH(ICO,JX,LJ,NE,NVAR,LBAND,NNOD)
      DIMENSION ICO(NE,1),JX(1),LJ(1)
      LBAND=0
      NV2=2*NVAR
      DO 3 I=1,NE
      DO 4 J=1,NVAR
      DO 4 K=1,NNOD
      K1=(K-1)*NVAR
      LJ(J+K1)=JX(NVAR*ICO(I,K)-NVAR+J)
    4 CONTINUE
      MAX=0
      MIN=1000
      NV3=NVAR*NNOD
      DO 8 J=1,NV3
      IF(LJ(J).EQ.0) GO TO 8
      IF(LJ(J)-MAX) 6,6,5
    5 MAX=LJ(J)
    6 IF(LJ(J)-MIN) 7,8,8
    7 MIN=LJ(J)
    8 CONTINUE
      NB1=MAX-MIN
      IF(NB1.GT.LBAND) LBAND=NB1
    3 CONTINUE
      RETURN
      END

E:LS--

   D       103B              .4     ID        0B              .5              608
            67B              .8      D       72B

-

-          112B ENTRY                          I          I        1263
I A          0B               VAR-DIM          J          I        1278
I A          0B                1               K          I        1238
I            130B                             LBAND      I A        0B
I A          0B                1              MAX        I        1258
I            124B                             NB1        I        1318
I A          0B                               NNOD       I A        0B
I A          0B                               NV2        I        1218
I            122B

M-UNIT LENGTH          23 SYMBOLS
ORAGE USED            .284 SECONDS
```

```
INE EXPAND      73/173  TS TRACE                                FTN 4.8+577          83/1

      SUBROUTINE EXPAND(AMODE,NAM,VV,JX,NDS,NVAR)
      DIMENSION VV(1),AMODE(1),JX(1)
      DO 5 I=1,NAM
      AMODE(I)=0.0
      IF(JX(I).EQ.0) GO TO 5
      AMODE(I)=VV(JX(I))
    5 CONTINUE
      WRITE(6,40)
      DO 10 I=1,NDS
      I2=NVAR*I
      I1=I2-NVAR+1
      WRITE(6,41) I,(AMODE(J),J=I1,I2)
   10 CONTINUE
   40 FORMAT(///,5X,"NODE",9X,"U-DISPL.",11X,"V-DISPL.",/)
   41 FORMAT(I7,8X,E12.6,5X,E12.6)
      RETURN
      END


    OUTCI.    OUTCR.    TAPE6#

ELS--

   D        21B              .10   ID         0B              .40   F        65B

-

 R A         0B              1     EXPAND     -          618B ENTRY
 I         107B                    I1         I         1118
 I         110B                    J          I         1128
 I A         0B              1     NAM        I A         0B
 I A         0B                    NVAR       I A         0B
 -              EXTERNAL.          OUTCR.     -                EXTERNAL.
 -              EXTERNAL.          VV         R A         0B                1

M-UNIT LENGTH          18 SYMBOLS

ORAGE USED           .123 SECONDS
```

```
INE PLACEZ     73/173  TS TRACE                    FTN 4.8+577        83/1

      SUBROUTINE PLACEZ(PP,C,CON,ICON,NCON,NN,LBAND)
      DIMENSION C(1),CON(1),PP(1),ICON(1)
      DO 18 I=1,NCON
      I1=ICON(I)
      I2=LBAND*(I1-1)+I1
      LC1=I1-LBAND
      IF(LC1.LE.0) LC1=1
      LC2=I1+LBAND
      IF(LC2.GT.NN) LC2=NN
      DO 17 J=LC1,LC2
      IF(I1-J) 9,10,10
   10 IJ=LBAND*(J-1)+I1
      GO TO 16
    9 IJ=LBAND*(I1-1)+J
   16 PP(J)=PP(J)-C(IJ)*CON(I)
   17 C(IJ)=0.00
   18 CONTINUE
      DO 25 I=1,NCON
      I1=ICON(I)
      I2=LBAND*(I1-1)+I1
      C(I2)=1.E08
      PP(I1)=1.E08*CON(I)
   25 CONTINUE
      RETURN
      END

ELS--

          448              .10          368              .16          518
   D      678              .25   ID      08

-

 R A       08         1          CON      R A       08         1
 I       1268                    ICON     I A       08         1
 I       1308                    I1       I       1318
 I       1278                    J        I       1338
 I A       08                    LC1      I       1258
 I       1328                    NCON     I A       08
 I A       08                    PLACEZ   -       1208 ENTRY
 R A       08         1

M-UNIT LENGTH          21 SYMBOLS

ORAGE USED          .296 SECONDS
```

```
      SUBROUTINE BAND(A,B,N,M,LT,DET)                                   BND
      DIMENSION A(1),B(1)                                               BND
      MM=M-1                                                            BND
      NM=N*M                                                            BND
      NM1=NM-MM                                                         BND
      IF (LT.NE.1) GO TO 55                                             BND
      MP=M+1                                                            BND
      KK=2                                                              BND
      FAC=DET                                                           BND
      A(1)=1./SQRT(A(1))                                                BND
      BIGL=A(1)                                                         BND
      SML=A(1)                                                          BND
      A(2)=A(2)*A(1)                                                    BND
      A(MP)=1./SQRT(A(MP)-A(2)*A(2))                                    BND
      IF(A(MP).GT.BIGL)BIGL=A(MP)                                       BND
      IF(A(MP).LT.SML)SML=A(MP)                                         BND
      MP=MP+M                                                           BND
      DO 62 J=MP,NM1,M                                                  BND
      JP=J-MM                                                           BND
      MZC=0                                                             BND
      IF(KK.GE.M) GO TO 1                                               BND
      KK=KK+1                                                           BND
      II=1                                                              BND
      JC=1                                                              BND
      GO TO 2                                                           BND
1     KK=KK+M                                                           BND
      II=KK-MM                                                          BND
      JC=KK-MM                                                          BND
2     DO 65 I=KK,JP,MM                                                  BND
      IF(A(I).EQ.0.)GO TO 64                                            BND
      GO TO 66                                                          BND
64    JC=JC+M                                                           BND
65    MZC=MZC+1                                                         BND
      ASUM1=0.                                                          BND
      GO TO 61                                                          BND
66    MMZC=MM*MZC                                                       BND
      II=II+MZC                                                         BND
      KM=KK+MMZC                                                        BND
      A(KM)=A(KM)*A(JC)                                                 BND
      IF(KM.GE.JP)GO TO 6                                               BND
      KJ=KM+MM                                                          BND
      DO 5 I=KJ,JP,MM                                                   BND
      ASUM2=0.                                                          BND
      IM=I-MM                                                           BND
      II=II+1                                                           BND
      KI=II+MMZC                                                        BND
      DO 7 K=KM,IM,MM                                                   BND
      ASUM2=ASUM2+A(KI)*A(K)                                            BND
7     KI=KI+MM                                                          BND
5     A(I)=(A(I)-ASUM2)*A(KI)                                           BND
6     CONTINUE                                                          BND
      ASUM1=0.                                                          BND
      DO 4 K=KM,JP,MM                                                   BN
4     ASUM1=ASUM1+A(K)*A(K)                                             BN
61    S=A(J)-ASUM1                                                      BN
      IF(S.LT.0.)DET=S                                                  BN
      IF(S.EQ.0.)DET=0.                                                 BN
```

```
INE BAND        73/173  TS TRACE                    FTN 4.8+577          83/12

      IF(S.GT.0.)GO TO 63                                                BNDF
      NROW=(J+MM)/M                                                      BNDF
      WRITE(6,99) NROW                                                   BNDF
99    FORMAT(35HOERROR CONDITION ENCOUNTERED IN ROW,I6)                  BNDF
      RETURN                                                             BNDF
63    A(J)=1./SQRT(S)                                                    BNDF
      IF(A(J).GT.BIGL)BIGL=A(J)                                          BNDF
      IF(A(J).LT.SML)SML=A(J)                                            BNDF
62    CONTINUE                                                           BNDF
      IF(SML.LE.FAC*BIGL)GO TO 54                                        BNDF
      GO TO 53                                                           BNDF
54    DET=0.                                                             BNDF
      RETURN                                                             BNDF
53    DET=SML/BIGL                                                       BND
55    B(1)=B(1)*A(1)                                                     BND
      KK=1                                                               BND
      K1=1                                                               BND
      J=1                                                                BND
      DO 8 L=2,N                                                         BND
      BSUM1=0.                                                           BND
      LM=L-1                                                             BND
      J=J+M                                                              BND
      IF(KK.GE.M)GO TO 12                                                BND
      KK=KK+1                                                            BND
      GO TO 13                                                           BND
12    KK=KK+M                                                            BND
      K1=K1+1                                                            BND
13    JK=KK                                                              BND
      DO 9 K=K1,LM                                                       BND
      BSUM1=BSUM1+A(JK)*B(K)                                             BND
      JK=JK+MM                                                           BND
9     CONTINUE                                                           BND
8     B(L)=(B(L)-BSUM1)*A(J)                                             BND
      B(N)=B(N)*A(NM1)                                                   BND
      NMM=NM1                                                            BND
      NN=N-1                                                             BND
      ND=N                                                               BND
      DO 10 L=1,NN                                                       BND
      BSUM2=0.                                                           BND
      NL=N-L                                                             BND
      NL1=N-L+1                                                          BND
      NMM=NMM-M                                                          BND
      NJ1=NMM                                                            BND
      IF(L.GE.M)ND=ND-1                                                  BND
      DO 11 K=NL1,ND                                                     BND
      NJ1=NJ1+1                                                          BND
      BSUM2=BSUM2+A(NJ1)*B(K)                                            BND
11    CONTINUE                                                           BND
10    B(NL)=(B(NL)-BSUM2)*A(NMM)                                         BND
      RETURN                                                             BND
      END                                                                BND
```

```
LINE PSET        73/173  TS TRACE                          FTN 4.8+577        83/12

                SUBROUTINE PSET(A,M)
                DIMENSION A(1)
                DO 1 I=1,M
              1 A(I)=0.00
                RETURN
                END
LS--
  ID          08

R A          08              1                    I          I          228
I A          08                                   PSET       -          168 ENTRY

-UNIT LENGTH                5 SYMBOLS
RAGE USED                .043 SECONDS
```

```
TINE PRESET     73/173  TS TRACE                    FTN 4.3+577     83/12

            SUBROUTINE PRESET(A,M,N)
            DIMENSION A(M,1)
            DO 1 I=1,M
            DO 2 J=1,N
          2 A(I,J)=0.00
          1 CONTINUE
            RETURN
            END

IELS--
   ID          08              .2    ID          08
--

 R A          08          VAR-DIM          I          I          36B
 I           37B                           M          I A         0B
 I A          0B                           PRESET     -          26B ENTRY

M-UNIT LENGTH          8 SYMBOLS
ORAGE USED          .060 SECONDS
```

```
UTINE MULT1      73/173  TS TRACE                    FTN 4.8+577        83/12

      SUBROUTINE MULT1(X,Y,S,Z,M1,M2,M3)
C
C     MULTIPLIES THE MATRICES  Y (TRANSPOSE) * X * Y .
C
      DIMENSION X(M1,1),Y(M1,1),Z(M3,1),S(M2,1)
      DO 1 I=1,M1
      DO 2 K=1,M2
      XX=0.00
      DO 3 J=1,M1
    3 XX=XX+X(I,J)*Y(J,K)
    2 Z(I,K)=XX
    1 CONTINUE
      DO 4 I=1,M2
      DO 5 K=I,M2
      XX=0.00
      DO 6 J=1,M1
    6 XX=XX+Y(J,I)*Z(J,K)
      S(I,K)=XX
    5 S(K,I)=XX
    4 CONTINUE
      RETURN
      END

ELS--

  ID      08          .2    ID      08          .3    ID      08
  ID      08          .6    ID      08

-

I       1278                        J       1308        I       1308
I       1318                        MULT1   1108 ENTRY  -       1108 ENTRY
I A       08                        M2        08        I A       08
I A       08                        S         08        R A       08          VAR-D
R A       08  VAR-DIM               XX      1328        R       1328
R A       08  VAR-DIM               Z         08        R A       08          VAR-D

M-UNIT LENGTH        18 SYMBOLS
IORAGE USED'        .264 SECONDS
```

```
      SUBROUTINE ISOPAR(X,Y,ST,FL,B,D,AN,ANS,ANT,H,GR,IS,IGR,ITRI)
      DIMENSION X(1),Y(1),ST(16,1),FL(1),B(3,1),D(3,1),AN(1),ANS(1),
     1ANT(1),W(3),XI(3),AK(16,16),C(3,16),AJ(2,2),AI(2,2)
      DATA W/0.555555555555556,0.888888888888889,0.555555555555556/
      DATA XI/-0.774596669224148,0.0,0.774596669224148/
      IF(IS.EQ.0) GO TO 1000
      CALL PRESET(ST,16,16)
      CALL PRESET(B,3,16)
      CALL PSET(FL,16)
      DO 26 I=1,3
      DO 27 J=1,3
      S=XI(I)
      T=XI(J)
      CALL SHAPE(AN,ANS,ANT,S,T,IGR,ITRI)
      CALL BMATRX(ANS,ANT,X,Y,B,AJ,AI,DET)
      CALL MULT1(D,B,AK,C,3,16,3)
      DET=H*DET
      DO 3 K=1,16
      DO 4 L=1,16
    4 ST(K,L)=ST(K,L)+(W(I)*W(J)*AK(K,L)*DET)
    3 CONTINUE
      IF(IGR.EQ.0) GO TO 27
      DET=GR*DET
      DO 5 K=1,8
      L=2*K
    5 FL(L)=FL(L)+(DET*W(I)*W(J)*AN(K))
   27 CONTINUE
   26 CONTINUE
 1000 RETURN
      END
```

```
     BMATRX     MULT1     PRESET     PSET     SHAPE
ELS--
  ID         OB               .4   ID          OB              .5    ID         OB
  D        140B            .1000              146B

R           226B           4               AJ       R         721B               4
R           241B           256             AN       R  A        0B               1
R   A         0B           1               ANT      R  A        0B               1
R   A         0B           3               BMATRX   R              SUBROUTINE
R           641B           48              D        R  A        0B               3
R           234B                           FL       R  A        0B               1
R   A         0B                           H        R  A        0B
I           725B                           IGR      I  A        0B
I   A         0B                           ISOPAR   -         151B ENTRY
I   A         0B                           J        I         232B
I           727B                           L        I         233B
```

```
IINE BONDRY     73/173  TS TRACE                          FTN 4.8+577          83/12.

      SUBROUTINE BONDRY(FL,X,Y,AN,ANS,ANT,H,IS,IB,IEL,ITRI)
      DIMENSION FL(1),X(1),Y(1),AN(1),ANS(1),ANT(1),W(3),XI(3),
     1PX(3),PY(3),JE(3)
      DATA W/0.55555555555556,0.88888888888889,0.55555555555556/
      DATA XI/-0.77459666924148,0.0,0.77459666924148/
      IF(IS.EQ.0) GO TO 1000
      CALL PSET(FL,16)
      IF(IB.EQ.0) GO TO 1000
      DO 1 L=1,IB
      READ(5,2) IE,(JE(I),I=1,3),COR
    2 FORMAT(4I5,F10.0)
      READ(5,3) PX(1),PY(1),PX(2),PY(2),PX(3),PY(3)
    3 FORMAT(6F10.0)
      JL=JE(1)
      JM=JE(2)
      JN=JE(3)
      DO 4 I=1,3
      IF(IE.NE.1) GO TO 5
      T=COR
      S=XI(I)
      CALL SHAPE(AN,ANS,ANT,S,T,1,ITRI)
      DXS=ANS(JL)*X(JL)+ANS(JM)*X(JM)+ANS(JN)*X(JN)
      DYS=ANS(JL)*Y(JL)+ANS(JM)*Y(JM)+ANS(JN)*Y(JN)
      DL=SQRT(DXS*DXS+DYS*DYS)
      GO TO 6
    5 S=COR
      T=XI(I)
      CALL SHAPE(AN,ANS,ANT,S,T,1,ITRI)
      DXT=ANT(JL)*X(JL)+ANT(JM)*X(JM)+ANT(JN)*X(JN)
      DYT=ANT(JL)*Y(JL)+ANT(JM)*Y(JM)+ANT(JN)*Y(JN)
      DL=SQRT(DXT*DXT+DYT*DYT)
    6 DO 7 J=1,3
      J2=2*JE(J)
      J1=J2-1
      ZZ=0.00
      XX=0.00
      DO 8 K=1,3
      XX=XX+DL*AN(JE(J))*(AN(JE(K)))*H*PX(K)*W(I)
    8 ZZ=ZZ+DL*AN(JE(J))*(AN(JE(K)))*H*PY(K)*W(I)
      FL(J1)=FL(J1)+XX
      FL(J2)=FL(J2)+ZZ
    7 CONTINUE
    4 CONTINUE
    1 CONTINUE
      WRITE(6,499) IEL
      WRITE(6,500) (FL(I),I=1,16)
 1000 RETURN
  499 FORMAT(//,5X,"LOAD VECTOR FOR ELEMENT NUMBER = ",I5,2X,"IS",/)
  500 FORMAT(8F15.7)
      END
```

```
LINE SHAPE      73/173  TS TRACE                          FTN 4.8+577        83/12

      SUBROUTINE SHAPE(AN,ANS,ANT,S,T,N,ITRI)
      DIMENSION AN(1),ANS(1),ANT(1)
      IF(N.EQ.0) GO TO 1
      AN(1)=-(1.00-S)*(1.00-T)*(1.00+S+T)/4.00
      AN(2)=-(1.00+S)*(1.00-T)*(1.00-S+T)/4.00
      AN(3)=-(1.00+S)*(1.00+T)*(1.00-S-T)/4.00
      AN(4)=-(1.00-S)*(1.00+T)*(1.00+S-T)/4.00
      AN(5)=(1.00-S*S)*(1.00-T)/2.00
      AN(6)=(1.00-T*T)*(1.00+S)/2.00
      AN(7)=(1.00-S*S)*(1.00+T)/2.00
      AN(8)=(1.00-T*T)*(1.00-S)/2.00
    1 ANS(1)=(1.00-T)*(2.00*S+T)/4.00
      ANS(2)=(1.00-T)*(2.00*S-T)/4.00
      ANS(3)=(1.00+T)*(2.00*S+T)/4.00
      ANS(4)=(1.00+T)*(2.00*S-T)/4.00
      ANS(5)=-S*(1.00-T)
      ANS(6)=(1.00-T*T)/2.00
      ANS(7)=-S*(1.00+T)
      ANS(8)=-(1.00-T*T)/2.00
      ANT(1)=(1.00-S)*(S+2.00*T)/4.00
      ANT(2)=(1.00+S)*(2.00*T-S)/4.00
      ANT(3)=(1.00+S)*(2.00*T+S)/4.00
      ANT(4)=(1.00-S)*(2.00*T-S)/4.00
      ANT(5)=-(1.00-S*S)/2.00
      ANT(6)=-T*(1.00+S)
      ANT(7)=(1.00-S*S)/2.00
      ANT(8)=-T*(1.00-S)
      IF(ITRI.EQ.0) GO TO 2
      DELH=(1.00-S*S)*(1.00-T*T)/8.00
      DELHS=-2.00*S*(1.00-T*T)/8.00
      DELHT=-2.00*T*(1.00-S*S)/8.00
      IF(N.EQ.0) GO TO 3
      AN(3)=AN(3)+AN(4)+AN(7)
      AN(1)=AN(1)+DELH
      AN(2)=AN(2)+DELH
      AN(5)=AN(5)-2.0*DELH
      AN(4)=0.00
      AN(7)=0.00
    3 CONTINUE
      ANS(3)=ANS(3)+ANS(4)+ANS(7)
      ANS(1)=ANS(1)+DELHS
      ANS(2)=ANS(2)+DELHS
      ANS(5)=ANS(5)-2.0*DELHS
      ANS(4)=0.00
      ANS(7)=0.00
      ANT(3)=ANT(3)+ANT(4)+ANT(7)
      ANT(1)=ANT(1)+DELHT
      ANT(2)=ANT(2)+DELHT
      ANT(5)=ANT(5)-2.0*DELHT
      ANT(4)=0.00
      ANT(7)=0.00
    2 RETURN
      END
```

```
TINE BMATRX     73/173  TS TRACE                              FTN 4.8+577          83/12.

      SUBROUTINE BMATRX(ANS,ANT,X,Y,B,AJ,AI,DET)
      DIMENSION ANS(1),ANT(1),X(1),Y(1),B(3,1),AJ(2,2),AI(2,2)
      CALL PRESET(AJ,2,2)
      DO 1 K=1,8
      AJ(1,1)=AJ(1,1)+ANS(K)*X(K)
      AJ(1,2)=AJ(1,2)+ANS(K)*Y(K)
      AJ(2,1)=AJ(2,1)+ANT(K)*X(K)
    1 AJ(2,2)=AJ(2,2)+ANT(K)*Y(K)
      DET=AJ(1,1)*AJ(2,2)-AJ(1,2)*AJ(2,1)
      IF(DET.EQ.0) DET=1.E-8
      AI(1,1)=AJ(2,2)/DET
      AI(1,2)=-AJ(1,2)/DET
      AI(2,1)=-AJ(2,1)/DET
      AI(2,2)=AJ(1,1)/DET
      DO 2 K=1,8
      K1=2*K-1
      B(1,K1)=AI(1,1)*ANS(K)+AI(1,2)*ANT(K)
      B(3,K1)=AI(2,1)*ANS(K)+AI(2,2)*ANT(K)
      B(2,K1+1)=B(3,K1)
    2 B(3,K1+1)=B(1,K1)
    3 RETURN
      END
```

PRESET

ELS--

ID	OB	.2	ID	OB	.3	140B	
R A	0B	4	AJ	R A	0B		4
R A	0B	1	ANT	R A	0B		1
R A	0B	3	BMATRX	-	143B	ENTRY	
R A	0B		K	I	1578		
I	160B		PRESET	R		SUBROUTINE	
R A	0B	1	Y	R A	0B		1

M-UNIT LENGTH 15 SYMBOLS

ORAGE USED .459 SECONDS

```
LINE SIGISO     73/173  TS TRACE                          FTN 4.8+577        83/12.

      SUBROUTINE SIGISO(X,Y,B,D,U,AN,ANS,ANT,M,N,ITRI)
      DIMENSION X(1),Y(1),B(3,1),D(3,1),U(1),AN(1),ANS(1),ANT(1),
     1STRAIN(3),STRESS(3),AJ(2,2),AI(2,2)
      CALL PRESET(B,3,16)
      AA=N-1
      BB=M-1
      DO 50 J=1,N
      CC=J-1
      S=-1.00+CC*2.00/AA
      DO 51 I=1,M
      DD=I-1
      T=-1.00+DD*2.00/BB
      IF(ITRI.EQ.1) GO TO 100
      CALL SHAPE(AN,ANS,ANT,S,T,1,ITRI)
      CALL BMATRX(ANS,ANT,X,Y,B,AJ,AI,DET)
      IF(DET.EQ.0) GO TO 55
      XX=0.00
      YY=0.00
      DO 4 K=1,8
      XX=XX+X(K)*AN(K)
    4 YY=YY+Y(K)*AN(K)
      XX=XX+1.E-8
      RATIO=YY/XX
      THETA=ATAN(RATIO)*180.00/3.1415926
      RADIUS=SQRT(XX*XX+YY*YY)
      DO 5 K=1,3
      ZZ=0.00
      DO 6 L=1,16
    6 ZZ=ZZ+B(K,L)*U(L)
    5 STRAIN(K)=ZZ
      DO 7 K=1,3
      ZZ=0.00
      DO 8 L=1,3
    8 ZZ=ZZ+D(K,L)*STRAIN(L)
    7 STRESS(K)=ZZ
      GO TO 101
   55 WRITE(6,54) J,I
      GO TO 51
  100 WRITE(6,53)
  101 CONTINUE
      WRITE(6,52) J,I,XX,YY,RADIUS,THETA,(STRESS(K),K=1,3)
   51 CONTINUE
   50 CONTINUE
      RETURN
   52 FORMAT(2I10,7E14.5)
   53 FORMAT(///,5X,"ELEMENT IS TRIANGULAR TRANSITIONAL ELEMENT -- IGNOR
     1E STRESS CONDITIONS",/)
   54 FORMAT(2I10,5X,"DETERMINATE IS 0.0, IGNORE STRESS CONDITIONS")
      END

ATAN       BMATRX     OUTCI.     OUTCR.     PRESET     SHAPE      SQRT       TAP
```

BIBLIOGRAPHY

[1] Broek, D., "Elementary Engineering Fracture Mechanics", Noordhoff International Publishing Co., Groninger, Neth. (1974).

[2] "Fracture, an Advanced Treatise: Vols. 1-8", Edited by H.Liebowitz, Academic Press, New York, N.Y. (1968-72).

[3] Knott, J. F., "Fundamentals of Fracture Mechanics", Butterworths, London (1973).

[4] Rolfe, S. T., "Fracture and Fatigue Control in Structures", Prentice-Hall, Englewood Cliffs, N.J. (1975).

[5] Sneddon, I., Lowengrub, M., "Crack Problems in the Classical Theory of Elasticity", John Wiley and Sons, New York, N.Y. (1969)

[6] Watwood Jr., V. B., "The Finite Element Method for Prediction of Crack Behaviour", Nuclear Engineering and Design 11, North Holland Pub. Co., Amsterdam, Neth.(1969)

[7] Chan, S. K., Tuba, I. S., Wilson, W. K., "On the Finite Element Method in Linear Fracture Mechanics", Eng'g. Fract. Mech., (2) (1970)

[8] Mowbray, D. F., "A Note on the Finite Element Method in Linear Fracture Mechanics", Eng'g. Fract. Mech., (2) (1970)

[9] Anderson, G. P., Ruggles, V. L., Stibor, G.S., "Use of Finite Element Computer Programs in Fracture Mechanics", Int. J. of Fract. Mech., V7, No.1 (1971).

[10] Parks, D. M., "A Stiffness Derivative Finite Element Technique for Determination of Crack Tip Stress Intensity Factors", Int. J. of Fract. V10, No. 4 (1974).

[11] Henshell, R. D., Shaw, K. G., "Crack Tip Finite Elements are Unnecessary", Int. J. for Num. Meth. in Eng'g. V9 (1975).

[12] Barsoum, R. S., "On the Use of Isoparametric Finite Elements in Linear Fracture Mechanics, Int. J. for Num. Meth. in Eng'g, V10 (1976)

[13] Mirza, F. A., Olson, M.D., "Energy Convergence and Evaluation of Stress Intensity Factory KI for Stress Singular Problems by Mixed Finite Element Method", Int. J. of Fract., V14, No. 6 (1978).

[14] Heymann, F. J., "A Review of the Use of Isoparametric Finite Elements for Fracture Mechanics", Engineering Applications of Fracture Mechanics, Pergammon Press, London (1980).

[15] Swedlow, J. L., "Crack Tip Finite Element Analyses", 'Fracture Mechanics' ed. by Perrone, Liebowitz, Mulville and Pilkey, Univ. Press of Virginia, Univ. of Virginia (1978).

[16] Hilton, P. D., Sih, G. C., "Application of the Finite Element Method to the Calculation of Stress Intensity Factors", 'Mechanics of Fracture 1- Methods of Analysis and Solution of Crack Problems' ed. G.C. Sih, Noordhof Int. Pub., Leyden, Neth. (1973).

[17] Tong, P., Atluri, S. N., "On Hybrid Finite Element Techniques for Crack Analysis", 'Fracture Mechanics and Technology 2' ed. G.C.Sih and C. L. Chow, Sijthoff and Noordhoff Int. Pub., Neth (1977).

[18] Mau, S. T., Yang, M. S., "Some Applications of a Hybrid Finite Element Method to Crack Problems", 'Fracture Mechanics and Technology 2' ed. G. C. Sih and C. L. Chow, Sijthoff and Noordhoof Int. Pub.,Neth. (1977)

[19] Griffith, A. A., "The Phenomena of Rupture and Flow in Solids", Proc. Roy. Soc., Series A (1920)

[20] Orowan, E., "Fracture and Strength of Solids: Report on Progress in Physics", Phys. Soc., London (1949).

[21] Irwin, G. R., "Fracture Dynamics, Fracturing of Metals", A.S.M. (1948).

[22] Sih, G. D., "Handbook of Stress Intensity Factors", Inst. of Fracture and Solid Mech., Lehigh Univ., Bethlehem, P.A. (1973).

[23] "The Surface Crack: Physical Problem and Computational Solutions", ed. J. L. Swedlow, A.S.M.E., New York, N. Y. (1972).

[24] Rice, J. R., "A Path Independent Integral and the Approximate Analysis of Strain Concentration by Notches and Cracks", J. of Appl. Mech. (1968)

[25] Leung, P.T.T., "Formulation of Transitional Elements and Applications to Linear Elastic Fracture Mechanics", Master of Engineering Thesis, McMaster Univ. (1982).

[26] Bathe, K.J., "Finite Element Procedures in Engineering Analysis", Prentice - Hall Inc., Englewood Cliffs, N.Y. (1982)

[27] Bowie, O.L., "Rectangular Tensile Sheet with Symmetric Edge Cracks", J. of Appl. Mech. (1964).

[28] Bowie, O.L., Neal, D.M., "A Note on the Central Crack in a Uniformly Stressed Strip", Eng'g. Fract. Mech., V2 (1970).

[29] Bowie, O.L., Freese, C.E., "Central Crack in Plane Orthotropic Rectangular Sheet", Int. J. of Fract. Mech., V8, No.1 (1972).

[30] "Standard Method of Test for Plane-Strain Fracture Toughness of Metallic Materials", ASTM Designation E 399-82, ASTM Annual Standards.

[31] "18Ni-Maraging Steel (250 Grade) Fracture Toughness Test Results", Supplied by Dr. D. W. Hoeppner, Univ. of Toronto (1983).

[32] Zienkiewicz, O.C., "The Finite Element Method in Engineering Science", McGraw Hill, London (1971).